Saettone *et al. Epigenetics & Chromatin (2018) 11:10*
https://doi.org/10.1186/s13072-018-0180-6

Epigenetics & Chromatin

RESEARCH

Open Access

The bromodomain-containing protein Ibd1 links multiple chromatin-related protein complexes to highly expressed genes in *Tetrahymena thermophila*

Alejandro Saettone[1], Jyoti Garg[2†], Jean-Philippe Lambert[3,6,7†], Syed Nabeel-Shah[1,8], Marcelo Ponce[4], Alyson Burtch[1], Cristina Thuppu Mudalige[1], Anne-Claude Gingras[3,5], Ronald E. Pearlman[2] and Jeffrey Fillingham[1*]

Abstract

Background: The chromatin remodelers of the SWI/SNF family are critical transcriptional regulators. Recognition of lysine acetylation through a bromodomain (BRD) component is key to SWI/SNF function; in most eukaryotes, this function is attributed to SNF2/Brg1.

Results: Using affinity purification coupled to mass spectrometry (AP–MS) we identified members of a SWI/SNF complex (SWI/SNF^{Tt}) in *Tetrahymena thermophila*. SWI/SNF^{Tt} is composed of 11 proteins, Snf5^{Tt}, Swi1^{Tt}, Swi3^{Tt}, Snf12^{Tt}, Brg1^{Tt}, two proteins with potential chromatin-interacting domains and four proteins without orthologs to SWI/SNF proteins in yeast or mammals. SWI/SNF^{Tt} subunits localize exclusively to the transcriptionally active macronucleus during growth and development, consistent with a role in transcription. While *Tetrahymena* Brg1 does not contain a BRD, our AP–MS results identified a BRD-containing SWI/SNF^{Tt} component, Ibd1 that associates with SWI/SNF^{Tt} during growth but not development. AP–MS analysis of epitope-tagged Ibd1 revealed it to be a subunit of several additional protein complexes, including putative SWR^{Tt}, and SAGA^{Tt} complexes as well as a putative H3K4-specific histone methyl transferase complex. Recombinant Ibd1 recognizes acetyl-lysine marks on histones correlated with active transcription. Consistent with our AP–MS and histone array data suggesting a role in regulation of gene expression, ChIP-Seq analysis of Ibd1 indicated that it primarily binds near promoters and within gene bodies of highly expressed genes during growth.

Conclusions: Our results suggest that through recognizing specific histones marks, Ibd1 targets active chromatin regions of highly expressed genes in *Tetrahymena* where it subsequently might coordinate the recruitment of several chromatin-remodeling complexes to regulate the transcriptional landscape of vegetatively growing *Tetrahymena* cells.

Keywords: Chromatin-remodeling complexes, Bromodomain, Tetrahymena

*Correspondence: Jeffrey.fillingham@ryerson.ca
†Jyoti Garg and Jean-Philippe Lambert contributed equally to this work
[1] Department of Chemistry and Biology, Ryerson University, 350 Victoria St., Toronto M5B 2K3, Canada
Full list of author information is available at the end of the article

Background

Eukaryotic cells possess multiple levels of regulation of mRNA transcription by RNA polymerase II. Many co-activators of transcription exert their function through chromatin-modifying activities. In budding yeast, the SAGA histone acetyl transferase complex co-activates transcription by acetylating specific lysine residues in the N-terminus of histone H3 within the nucleosome, which can then serve as a platform to recruit the SWI/SNF complex via the bromodomain (BRD) present in SNF2/Brg1 [1]. The BRD specifically binds acetyl-lysine (Kac) within proteins such as histones [2]. When recruited to a genomic region, the SWI/SNF complex co-activates transcription in part by hydrolyzing ATP via the Snf2 subunit and remodeling nucleosomes to make promoter sequences available to be bound by general transcription factors (TFs) such as TFIID. Some other histone-modifying complexes that function in promoting transcription include the NuA4 histone acetyl transferase that acetylates nucleosomal H4 [3], and the Set1 and Set2 histone methyl transferases that methylate nucleosomal H3K4 and H3K36 [4], respectively. Additional protein domains that function in transcription complexes by recognizing some of the diverse histone post-translational modifications (PTMs) include the methyl lysine-recognizing PHD and chromodomains [5]. Other ATP-dependent chromatin-remodeling complexes that function in transcription include the SWR complex that exchanges core H2A in the nucleosome for the transcription-friendly histone H2A variant Htz1 [6, 7] and the INO80 complex one function of which is to catalyze the reverse reaction [8].

A typical eukaryotic nucleus is composed of regions of transcriptionally inert heterochromatin as well as euchromatic areas which are considered competent for transcription. The ciliate protozoan *Tetrahymena thermophila* is a unique model system for studying transcription since it segregates germ-line-specific silent (micronucleus—MIC), and somatic transcriptionally active (macronucleus—MAC) chromatin into two distinct nuclei contained within its single cell. The different chromatin structures of the MAC and MIC have their origins in the sexual phase (conjugation) of the life cycle [9]. After pairing, the MIC in each of the two cells undergoes meiosis, generating four haploid meiotic products, only one of which is retained. This gametic nucleus divides mitotically, and one of the two resulting identical haploid nuclei is reciprocally exchanged and fuses with that of its partner to form a genetically identical diploid zygotic nucleus in each cell. The zygotic nucleus divides twice, resulting in four identical products at which point two begin to develop into new MACs (NM). MAC development in the NM of each exconjugant involves extensive programmed DNA rearrangements/irreversible genome silencing that is directly linked to ncRNA-based changes in chromatin structure. These DNA rearrangements include site-specific chromosome fragmentation as well as the deletion of MIC-limited sequences called internal eliminated sequences (IESs) that together result in the loss of ~15% of the germ-line genome [10]. IES deletion begins with the bidirectional transcription of RNAs from the meiotic MIC [11, 12]. Meiosis is the only stage of the *Tetrahymena* life cycle where the MIC is transcribed [11, 13]. This meiotic MIC-specific transcription is catalyzed by RNAPII [13]. A global MIC-specific nuclear run-on analysis showed that meiotic MIC-specific transcription is biased toward IES DNA, implying that initiation/start-site selection of the MIC-specific transcription is regulated and not simply a result of global or random transcription [12, 14]. The underlying molecular mechanisms underlying any transcription in *Tetrahymena* remain poorly understood.

We previously characterized a SNF2-related gene in *T. thermophila* [15]. Despite high primary sequence similarity of Brg1^{Tt} to the budding yeast Snf2 and human Brg1 through most of the protein, Brg1^{Tt} does not possess a recognizable BRD, and its C-terminal region, unlike the entire protein, is dispensable for growth and development [15] raising the possibility that SWI/SNF^{Tt} functions independently of histone acetylation. Here we report a unique BRD-containing protein, Ibd1, which is a component of SWI/SNF^{Tt} during vegetative growth but not during conjugation. Recombinant Ibd1 recognizes several Kac marks on histones that are correlated with active transcription in *Tetrahymena*. AP–MS analysis of Ibd1 revealed it to interact with protein complexes in addition to SWI/SNF^{Tt} including SWR^{Tt}, SAGA^{Tt}, as well as with a novel putative H3K4-specific histone methyltransferase. ChIP-Seq analysis of Ibd1 suggests a role for the protein during transcription. We suggest that Ibd1 coordinates high levels of transcription of highly expressed genes in *T. thermophila*.

Results

Identification of *T. thermophila* SWI/SNF complex

We previously cloned and characterized the Snf2/Brg1 ortholog in *T. thermophila* [15] and predicted it to be a component of a SWI/SNF complex, similar to the situation in *Saccharomyces cerevisiae* [16] and human cells [17]. We used an affinity purification coupled to mass spectrometry (AP–MS) to identify *T. thermophila* SWI/SNF. Specifically, we profiled and compared the set of interacting proteins of two distinct putative SWI/SNF^{Tt} components, Snf5^{Tt} (TTHERM_00304150), a core subunit of yeast and human SWI/SNF complexes [18], and Snf5^{Tt}-interacting protein Saf5^{Tt} (TTHERM_00241840). Our comparative sequence analysis shows Snf5^{Tt} to be

highly similar to that of yeast and animal cells across most of the protein (see Additional file 1). We generated stable *T. thermophila* cell lines expressing FZZ epitope-tagged *SNF5*^{Tt} and *SAF5*^{Tt} from their respective macronuclear chromosomal loci by homologous recombination-mediated gene replacement [19]. The FZZ epitope tag contains two protein A moieties and one 3xFLAG separated by a TEV cleavage site [20], permitting tandem affinity purification of an FZZ fusion protein, which permits subsequent analysis of co-purifying proteins by Western blotting and/or mass spectrometry [21]. The *SNF5*^{Tt}*-FZZ* and *SAF5*^{Tt}*-FZZ* tagging constructs (see Additional files 1, 2) were used to transform growing *T. thermophila* strains using biolistic transformation. Gene replacement of the WT *SNF5*^{Tt} and *SAF5*^{Tt} that occurs by homologous recombination [22] and 'phenotypic assortment' (reviewed in [23]) generates homozygosity in the polyploid MAC for the chromosome containing the *SNF5*^{Tt}*-FZZ* or *SAF5*^{Tt}*-FZZ* gene locus. Western blotting using an FZZ-specific antibody demonstrated expression of the epitope-tagged Snf5^{Tt} or Saf5^{Tt} in whole-cell extracts from Snf5^{Tt}-FZZ- and Saf5^{Tt}-FZZ-expressing strains, respectively (Fig. 1a, left panel, lanes 2 and 4; b, lanes 3 and 4) compared to that of untagged strains (Fig. 1a, left panel, lanes 1 and 3; b, lanes 1 and 2). Indirect immunofluorescence on Snf5^{Tt}-FZZ and Saf5^{Tt}-FZZ in growing *T. thermophila* showed localization to the transcriptionally active MAC and not to the silent MIC (Fig. 1c), identical to what we observed previously for Brg1^{Tt} [15], consistent with the hypothesis that Snf5^{Tt} and Saf5^{Tt} are a member of a Brg1^{Tt}-containing SWI/SNF^{Tt}. A Brg1^{Tt}-specific antibody [15] demonstrated co-purification of Brg1^{Tt} with Snf5^{Tt}-FZZ and Saf5^{Tt}-FZZ affinity purified from whole-cell extracts from Snf5^{Tt}-FZZ expressing (Fig. 1a, lanes 3–6) and Saf5^{Tt}-FZZ expressing (Fig. 1b) but not from untagged strains during vegetative growth.

We next performed a gel-free LC–MS/MS-based analysis for each of Snf5-FZZ and Saf5^{Tt}-FZZ of the respective affinity purifications to define their sets of interacting proteins. To provide statistical rigor to our AP–MS analyses, all interaction data were filtered using Significance Analysis of INTeractome express (SAINTexpress) which uses semiquantitative spectral counts to assign a confidence value to individual protein–protein interactions [24]. Application of SAINTexpress to the AP–MS data for two biological replicates of Snf5^{Tt}-FZZ and Saf5^{Tt}-FZZ affinity purifications from vegetatively growing *T. thermophila* filtered against numerous control AP–MS experiments revealed sets of interaction partners that pass the cutoff confidence value and are listed in Table 1. Our previous analysis [15] of the sequenced *T. thermophila* MAC genome predicted the existence of three potential SWI/SNF proteins in addition to Brg1^{Tt} and Snf5^{Tt}: Swi1^{Tt} (TTHERM_00243900), Swi3^{Tt} (TTHERM_00584840) and Snf12^{Tt} (TTHERM_00925560). The SAINTexpress analysis of the MS data for Snf5^{Tt}-FZZ and Saf5^{Tt}-FZZ (Table 1) revealed the identification of the respective baits and each other, in addition to Brg1^{Tt}, consistent

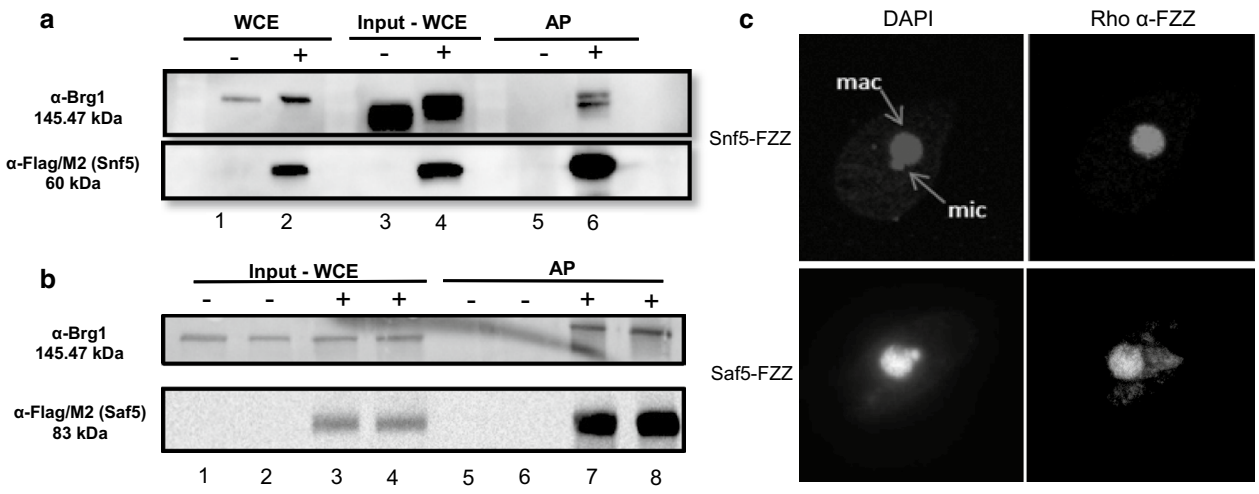

Fig. 1 Identification and affinity purification (AP) of Snf5 and Saf5: α-FLAG/M2 recognizes the FLAG tag on FZZ in the whole-cell extract (WCE) and AP experiments. **a** Expression analysis/AP of Snf5-FZZ. Snf5 ~60 kDa (18 kDa FZZ + 42 kDa Snf5). Lanes 1, 3 and 5 are untagged (−), and lanes 2, 4 and 6 are tagged (+, SNF5-FZZ) *Tetrahymena* strains. Lanes 1 and 2 represent WCE prepared with TCA precipitation. Lanes 3–6 were extracted with a soluble-affinity buffer. Some protein degradation is apparent. Snf5 co-purifies with Brg1 (top panel, lane 6), **b** expression analysis/AP of Saf5-FZZ. Saf5 ~83 kDa (18 kDa FZZ + 65 kDa Saf5). Lanes 1, 2, 5 and 6 are untagged (−), and lanes 3, 4, 7, 8 and 9 (positive control) are tagged (+, SAF5-FZZ) *Tetrahymena* strains. Saf5 co-purifies with Brg1 (top panel, lanes 7 and 8); **c** Snf5 and Saf5 localize to the MAC during growth. Left panels show stained nuclei, macronucleus (MAC) and micronucleus (MIC), by DAPI. Right panels show localization of the FZZ during vegetative growth

Table 1 AP–MS data for Snf5-FZZ and Saf5-FZZ uncover predicted and novel members of a *Tetrahymena* SWI/SNF complex

TTHERM	Gene name	Spectral count sum Snf5 (BAIT)	Spectral count sum Saf5 (BAIT)	SWI/SNF yeast ortholog	SWI/SNF human ortholog	Notes
TTHERM_00584840	*SWI3*	308	835	Swi3	BAF170/SMARCC2	–
TTHERM_01245640	*BRG1*	264	384	Snf2	BRM/SMARCA2	SNF2 catalytic subunit
TTHERM_00243900	*SWI1*	140	171	Swi1	BAF250A/ARID1A	–
TTHERM_00304150	*SNF5*	133	72	Snf5	BAF47/SMARCB1	–
TTHERM_00925560	*SNF12*	94	137	Snf12	SMARCD2	–
TTHERM_00092790	*SAF1*	85	78	–	–	Transmembrane protein, putative
TTHERM_00346460	*SAF2*	136	97	–	–	Hypothetical protein—13% glutamine
TTHERM_00129650	*SAF3*	79	40	–	–	Hypothetical protein—26% glutamine
TTHERM_00637690	*SAF4*	32	84	–	–	Hypothetical protein—31% glutamine
TTHERM_00241840	*SAF5*	64	56	–	BAF45a	PHD finger-containing protein
TTHERM_00729230	*IBD1*	48	107	–	–	Bromodomain-containing protein
TTHERM_00006320	Tetrin A	33	–	–	–	–

Curated SAINTexpress data from 2 biological replicates of SNF5-FZZ and SAF5-FZZ AP–MS samples. Genes in italics were previously predicted to be SWI/SNF components [15]. Saf (SWI/SNF-associated factor), Ibd (Interactive Bromodomain Protein). The members of the SWI/SNF complex are the first 11 rows

with Fig. 1a, b, Swi1^{Tt}, Swi3^{Tt} and Snf12^{Tt} (Table 1). Saf5^{Tt} possesses two tandem plant homeodomains (PHD domain). One known function of PHD domains is to mediate specific interactions with methylated lysine on histone proteins to positively regulate transcription [25]. PHD domain-containing proteins are not known to be present in core yeast SWI/SNF but are observed in several animal SWI/SNF complexes [26]. The two PHD domains of Saf5^{Tt} are in the same position and are highly similar to those of zebrafish DPF3 and mammalian proteins mBAF45a and hBAF45a (see Additional file 2) both of which are members of a cell type-specific SWI/SNF complex [26, 27]. DPF3 is part of the BAF chromatin-remodeling complex in zebrafish, and it is involved in regulation of muscle development and recognizes histones carrying both specific histone acetylation and methylation marks [27]. Snf5^{Tt}-FZZ additionally co-purified tetrin A (TTHERM_00006320), an insoluble cytoskeletal protein unique to ciliates [28]. We have previously noted a variable affinity of the M2 anti-FLAG antibody for this protein as was previously observed for other cytoskeletal proteins [29] and therefore decided not to follow-up on it here. Both Snf5^{Tt}-FZZ and Saf5^{Tt}-FZZ co-purified with 5 other proteins with no clear orthologs in other described SWI/SNF complexes. The first of these 5 proteins, Saf1 (SWI/SNF-associated factor 1, Table 1), is predicted to have a coiled coil and a transmembrane domain. Saf1 appears to have a homolog in *Paramecium tetraurelia* (XP_001441480.1) that also possesses the coiled coil domain but not a transmembrane domain. The next 3 proteins, Saf2^{Tt}, Saf3^{Tt} and Saf4^{Tt}, are *T. thermophila*-specific, meaning that they do not have identifiable known homologs in any other organism. However, all three possess clusters of glutamines in their primary sequence suggestive of a role in transcription [30]. The fifth protein SAINTexpress analysis revealed to co-purify with Snf5^{Tt}-FZZ and Saf5^{Tt}-FZZ is TTHERM_00729230 (Table 1), which possesses a canonical BRD. We named this protein Ibd1 (Interactive BromoDomain Protein 1). We suggest the 11 proteins Swi1^{Tt}, Swi3^{Tt}, Snf5^{Tt}, Snf12^{Tt}, Brg1^{Tt} and Ibd1 in addition to Saf1-5^{Tt} and together define the first known ciliate SWI/SNF complex.

Ibd1- and BRD-containing proteins in *T. thermophila*

The BRD is highly conserved across eukaryotic species, present in functionally diverse proteins including histone acetyl transferases (HATs), ATP-dependent chromatin-remodeling complexes, helicases, methyl transferases and transcriptional regulators [31]. Dysfunctional BRD-containing proteins have previously been linked to the development of several human pathologies and are now actively pursued as therapeutic targets [32]. Our finding

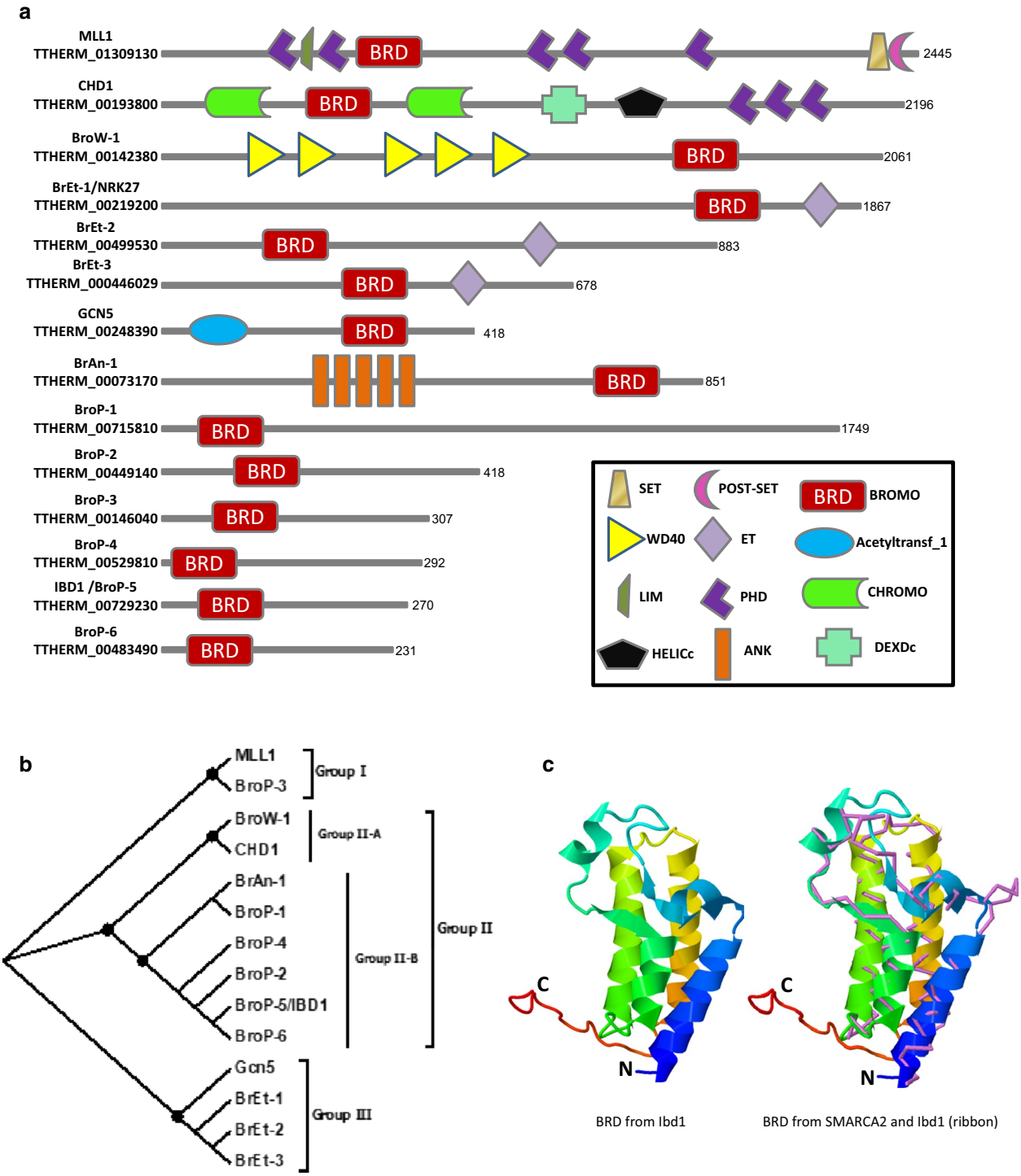

Fig. 2 Analysis of *Tetrahymena* BRD-containing proteins**. a** Domain architecture of the identified BRD-containing proteins. Domains were predicted using the SMART web tool and Pfam domain analysis (see "Methods"), **b** phylogenetic analysis of *Tetrahymena* BRDs. The amino acid sequences of the predicted BRDs were aligned using MUSCLE. The phylogenetic analysis was carried out using the neighbor joining method with 1000 bootstrap replicas (confidence > 90% for all nodes), **c** predicted structure (left) of the Ibd1 BRD shown in ribbon diagram with rainbow color scheme. Blue represents the N-terminus, whereas red shows the C-terminus of the predicted structure. The superimposition (right) was carried out using the BRD of human SMARCA2 protein (PDB: 5DKC) which is shown in violet color backbone format. *Note* The identified *Tetrahymena* BRD-containing proteins were named based on the domain architecture if no clear human ortholog was available. BroW1, bromo-WD40 domain protein; BrEt, bromo-Et domain protein; BrAn, Bomo-Ank domain protein; Brop1–6, BRD-containing protein

that a unique BRD-containing protein co-purifies with Snf5^{Tt}-FZZ and Saf5^{Tt}-FZZ prompted us to determine the full repertoire of BRD-containing proteins in *Tetrahymena*. Our query for BRDs in the *Tetrahymena* genome database, www.ciliate.org [33], identified 14 proteins (Fig. 2a). Consistent with human BRD-containing proteins [34], the *Tetrahymena* putative BRD-containing proteins appear functionally diverse and their BRDs can be found in combination with a variety of other domains (Fig. 2a). However, unlike humans and yeast, where multiple BRDs can be present within the same protein [34, 35], the *T. thermophila* BRDs are present as single copy. To classify the *T. thermophila* BRD-containing proteome, we carried out a phylogenetic analysis and categorized the set of proteins into three groups based on their BRD similarity (Fig. 2b). 'Group I' contains two proteins, Mll1 and BroP-3. The 'Group II' (Fig. 2b) can be further categorized into two subgroups such that 'Group II-A' contains only two proteins including Chd1^{Tt} and BroW1^{Tt}, whereas 'Group II-B' has six proteins including Snf5^{Tt}-interacting Ibd1 (or BroP5; see figure legend for nomenclature). Five out of the 6 proteins found in 'Group II-B' contain no recognizable domains other than BRDs (Fig. 2a, b). The similarities in the domain architecture and grouping pattern suggest that the 'Group II-B' proteins (which includes Ibd1) might be functionally more similar to each other than to those found within the other groups. Group III contains four proteins including Gcn5^{Tt} and three proteins that possess an ET (extra-terminal) domain in addition to a BRD. In many eukaryotes, including yeast and humans, bromodomain proteins containing two BRDs followed by an ET domain are referred to as the BET protein family [36]. BRDs generally function to recognize Kac motifs on histones or non-histone proteins to regulate various cellular processes including transcription [34]. The ET domains in contrast are thought to recruit effector proteins which in turn can regulate the transcriptional activity [37]. Structural conservation of a protein often yields insights into its functions. To gain insight into the function of Ibd1, we predicted the three-dimensional structure of its BRD and observed that it folds similarly to the known BRD structures. For example, the predicted structure can be superimposed to the C-terminal BRD of human SMARCA2 (Fig. 2c). This suggests that the Ibd1 protein may have a similar function in transcription to that of canonical SNF2 proteins in the yeast and animal SWI/SNF complex through recognition of a similar/same Kac substrate in histones.

Ibd1 recognizes Kac and interacts with multiple chromatin-related proteins

Our finding of a distinct BRD-containing protein in SWI/SNF^{Tt} is consistent with the fact that a BRD in the catalytic subunit (Snf2/Brg1) has important functions in eukaryotic SWI/SNF complexes. We aligned the primary sequence of the BRD of Ibd1 to those of Gcn5^{Tt}, yGcn5p, yBDF1, yBDF2 and ySWI2/SNF2 which are functional BRD-containing proteins (see Additional file 3). The alignment showed a number of conserved amino acids in the BRD including the highly conserved asparagine (N) that makes contact with Kac [34, 38], suggesting that Ibd1 as other BRD-containing proteins is likely to bind this mark. We expressed, purified and incubated recombinant 6xHIS-Ibd1 with a commercially available peptide array that includes a large number of possible histone post-translational modifications, including many histone acetylation sites. Recombinant 6xHIS-Ibd1 displayed strong specificity for acetylated H3K9 and H3K14, acetylated H2AK9 and H2AK13 and tri-acetylated H4K5, H4K8 and H4K12 (Table 2; see Additional file 4 for Raw Data), which are all acetylation patterns associated with the transcriptionally active MAC in *T. thermophila* [39, 40]. When incubated on the same peptide array, control recombinant histone methyltransferase 6xHIS-G9a recognized mono- and di-methylated H3K9 (Table 2; see Additional file 4 for Raw Data), as previously demonstrated [41].

We generated a stable line expressing Ibd1-FZZ from its MAC locus. The *IBD1-FZZ* tagging construct (see Additional file 2) was used to transform growing *T. thermophila* strains using biolistic transformation. After selection and phenotypic assortment, Western blotting demonstrated expression of Ibd1-FZZ in whole-cell extracts of transformed strains (Fig. 3a). Similar to Snf5^{Tt}-FZZ, Ibd1-FZZ also co-purifies with Brg1^{Tt} as assessed by Western blotting of affinity-purified material (Fig. 3b). Gel-free LC–MS/MS-based analysis on affinity-purified proteins identified 28 high-confidence Ibd1-FZZ co-purifying proteins (Table 3). Comparison of the interaction partners recovered from the purification of Snf5^{Tt}-FZZ, Saf5^{Tt}-FZZ and Ibd1-FZZ-interacting proteins (Fig. 3c; Table 3), showed 11 common proteins that co-purify with Ibd1, Saf5^{Tt} and Snf5^{Tt} including Swi1^{Tt}, Swi3^{Tt}, Snf5^{Tt}, Snf12^{Tt} and Brg1^{Tt}, Ibd1 and Saf1-5^{Tt} that together we hypothesize from a putative *T. thermophila* SWI/SNF complex.

The other 17 high-confidence Ibd1-interacting proteins (Fig. 3c; Table 3) could be divided into three groups, based on similarity to predicted *S. cerevisiae* orthologs: 1 the SAGA^{Tt} histone acetyl transferase co-activator complex containing Gcn5^{Tt}, Ada2^{Tt} and a PhD-containing protein, designated Aap1^{Tt} (Ada2-associated protein 1), 2 the SWR^{Tt} ATP-dependent chromatin-remodeling complex that in yeast and human cells deposits histone variant Htz1/H2A.Z onto chromatin (Swr1^{Tt}, Yaf9^{Tt}, Rvb1^{Tt}, RvB2^{Tt}, Swc2^{Tt} and Swc4^{Tt}), Swc5^{Tt} (C-terminal BCNT domain), two actin-like and three predicted

Table 2 Histone peptide-array data reveal the top post-translational modification recognized by Ibd1

Histone	Modification 1	Modification 2	Modification 3	Modification 4	Intensity average 6xHIS-Ibd1 (4 repetitions)	Intensity average 6xHIS-G9a (2 repetitions)
H3	*K9ac*	*K14ac*			*0.95*	0.02
H2a	K5ac	*K9ac*	*K13ac*		*0.92*	0.01
H4	***R3me2s***	*K5ac*	*K8ac*	*K12ac*	*0.90*	0.00
H4	*K5ac*	*K8ac*	*K12ac*	K16ac	*0.89*	0.03
H3	K9me3	*K14ac*			*0.88*	0.01
H3	S10P	*K14ac*			*0.88*	0.04
H4	*K5ac*	*K8ac*	*K12ac*		*0.84*	0.01
H3	T11P	*K14ac*			*0.82*	0.01
H2a	S1P	K5ac	*K9ac*	*K13ac*	*0.82*	0.01
H2a	S1P	*K9ac*	*K13ac*		*0.81*	0.01
H3	R2me2s	K4me2	R8me2a	*K9me2*	0.19	*0.96*
H3	R2me2a	K4me1	R8me2a	*K9me2*	0.18	*0.94*
H3	R2me2a	K4me2	R8me2a	*K9me2*	0.18	*0.90*
H3	K4ac	R8me2s	*K9me1*		0.21	*0.84*
H3	R2me2a	K4me2	R8me2a	*K9me1*	0.19	*0.83*
H3	R2me2a	K4me3	R8me2a	*K9me2*	0.18	*0.80*
H3	R2me2a	K4ac	R8me2a	*K9me2*	0.28	*0.79*
H3	R2me2a	K4me3	R8me2a	*K9me1*	0.19	*0.79*
H3	R2me2s	K4ac	R8me2a	*K9me1*	0.16	*0.76*
H3	R2me2s	K4me2	R8me2s	*K9me1*	0.17	*0.76*

The histone peptide array contains human histone modifications that resemble *Tetrahymena*'s histones. The intensity average columns show the top 10 histone modifications recognized by 6xHIS-Ibd1 and 6xHIS-G9a in italics. Bold italics means that the amino acid is not present in the *Tetrahymena*'s histone (see Additional file 4 for Raw Data)

Swc4-associated proteins (Sap1-3)^{Tt}, one of which possess an AT-hook (Sap1^{Tt}), the other two (Sap2^{Tt} and Sap3) contain no recognizable domains, and 3 a putative H3K4 methyl transferase (Atrx3/Set1-like). Sap3^{Tt} shares similarity only on a small portion of the protein with hypothetical proteins in *P. tetraurelia* and *Pseudocohnilembus persalinus.* Sap4^{Tt} shares similarity throughout the entire protein with a hypothetical protein in *P. persalinus.* The Ibd1 protein therefore appears to be a component of several chromatin-remodeling complexes (SWI/SNF^{Tt}, SAGA^{Tt}, SWR^{Tt}) and one containing an Atrx3/Set1-like HMT.

To further delineate the Ibd1 protein interaction network, we generated separate stable lines expressing Ada2^{Tt}-FZZ and Swc4^{Tt}-FZZ from their respective MAC loci following an identical strategy as outlined above. SAINTexpress analysis of AP–MS data from growing cells showed that Ada2^{Tt} co-purifies with Ibd1 in addition to the Ibd1-interacting Aap1^{Tt} and Gcn5^{Tt}. Additionally, Ada2^{Tt} co-purified with three PHD domain-containing proteins (Aap2^{Tt}, Aap3^{Tt} and Aap4^{Tt}; Fig. 3c; Table 3) and four *T. thermophila*-specific hypothetical proteins (Aap5^{Tt}, Aap6^{Tt}, Aap7^{Tt} and Aap8^{Tt}; Fig. 3c; Table 3) that we did not find to co-purify with Ibd1-FZZ. We suggest that the Ada2-interacting proteins together represent a *Tetrahymena* SAGA^{Tt} complex (Fig. 3c; Table 3).

SAINTexpress analysis of Swc4^{Tt}-FZZ AP–MS revealed it to co-purify a subset of Ibd1-interacting proteins that were predicted to be SWR^{Tt} complex proteins (Fig. 3c; Table 3). Swc4^{Tt}-FZZ further interacts with *T. thermophila* orthologs of the Tra1 and Tra2 PI3 kinases (Fig. 3c; Table 3), neither of which co-purified with Ibd1. In yeast, Swc4 co-purifies with Tra1 via the NuA4 histone acetyltransferase complex of which Swc4 is a component, in addition to SWR-C. We did not observe Swc4^{Tt}-FZZ to co-purify with any protein that would indicate it to be a member of a *T. thermophila* NuA4 complex. The set of proteins that we hypothesize to constitute SWR^{Tt} are listed in Table 3. Although the *T. thermophila* genome encodes a predicted ortholog of Swc6/Vps71 (TTHERM_01298590), we did not find it to co-purify with Swc4^{Tt} or Ibd1 in growing cells.

Ibd1 function during conjugation

To gain further insight into Ibd1 function, we assessed its expression through growth and sexual development. We performed Western blotting of whole-cell extracts made at different times during the *T. thermophila* life cycle, probing for Ibd1-FZZ (Fig. 4a, lower panel). We have previously demonstrated Brg1^{Tt} to have relatively constant levels of expression throughout growth and development

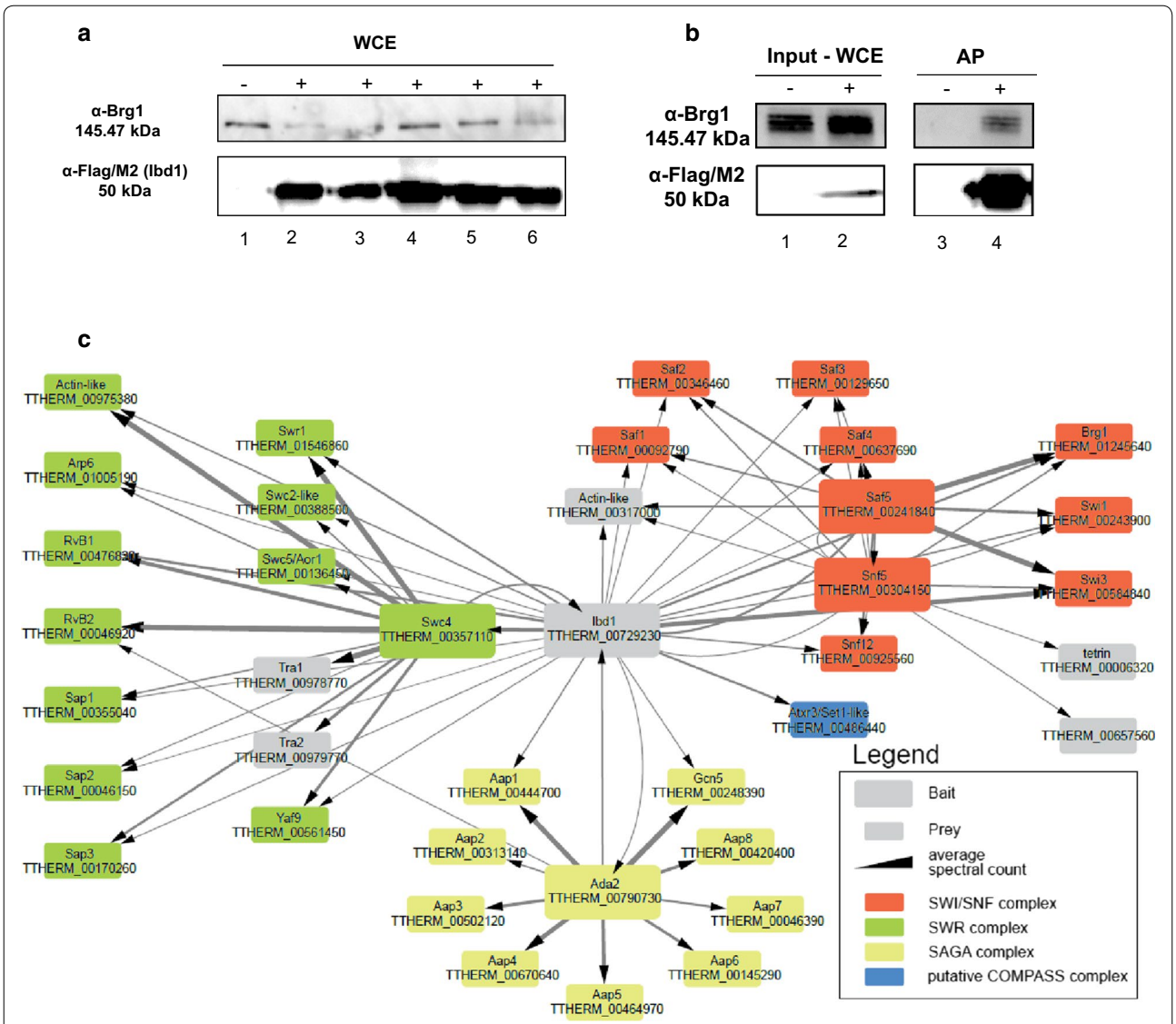

Fig. 3 Identification and affinity purification (AP) of Ibd1. **a** Western blot to assess whether *Tetrahymena* transformant cells are expressing Ibd1-FZZ. Whole-cell extract (WCE) using TCA of Ibd1-FZZ cells during vegetative growth. Ibd1 ~ 50 kDa (18 kDa FZZ + 32 kDa Ibd1). Lane 1 is untagged (−), and lanes 2, 3, 4, 5 and 6 are tagged (+, Ibd1-FZZ) *Tetrahymena* strains, **b** expression analysis of Ibd1-FZZ during vegetative growth. WCE and AP experiment extracted with a soluble-affinity buffer for untagged (−, lanes 1 and 3) and tagged (+, lanes 2 and 4) Ibd1-FZZ *Tetrahymena* strains. The BDR-containing protein is recognized by α-FLAG/M2 and co-purifies with Brg1 (right top panel, lane 4), **c** network view of Ibd1 protein–protein interactions. The edge thickness represents the averaged spectral counts for the prey. Bait proteins are shown in larger nodes which are colored according to predicted complexes as indicated

[15]. We therefore used anti-Brg1^{Tt} as a loading control (Fig. 4a, top panel) and anti-Pdd1 [42] as a development-specific control (Fig. 4a, middle panel) for these experiments. Similar to Brg1^{Tt}, Ibd1 is expressed throughout the *T. thermophila* life cycle. Indirect immunofluorescence of Ibd1-FZZ performed on growing and conjugating cells (Fig. 4b) demonstrated localization exclusively to the MAC during growth and conjugation, specifically to the parental MAC through early nuclear development including meiosis (Fig. 4b: 0–6 h) before switching to the anlagen midway through sexual development (Fig. 4b: 8 h). This is similar to what was shown previously for Brg1^{Tt} [15]. In particular, as for Brg1^{Tt}, localization of Ibd1-FZZ in the parental macronucleus is lost at the onset of macronuclear development, a stage where the two anterior nuclei (the anlagen) have become visibly larger than the posterior nuclei (Fig. 4b Ibd1-FZZ cells, compare 8 and 6 h post-mixing). The cellular localization

Table 3 AP–MS data for Ibd1-FZZ, Ada2-FZZ and Swc4-FZZ purified from vegetative cells

TTHERM	Gene name	Spectral count sum Ibd1 (BAIT)	Spectral count sum Swc4 (BAIT)	Spectral count sum Ada2 (BAIT)	Possible complex	Notes
TTHERM_00729230	*IBD*1	827	99	58	All listed below	Bromodomain-containing protein
TTHERM_00486440	Atxr3/*SET1*-like	125	–	–	COMPASS	–
TTHERM_00584840	*SWI*3	411	–	–	SWI/SNF	–
TTHERM_01245640	*BRG*1	202	–	–	SWI/SNF	SNF2 catalytic subunit
TTHERM_00925560	*SNF*12	81	–	–	SWI/SNF	–
TTHERM_00243900	*SWI*1	92	–	–	SWI/SNF	–
TTHERM_00304150	*SNF*5	64	–	–	SWI/SNF	–
TTHERM_00092790	*SAF*1	47	–	–	SWI/SNF	Transmembrane protein, putative
TTHERM_00346460	*SAF*2	39	–	–	SWI/SNF	Hypothetical protein—13% glutamine
TTHERM_00637690	*SAF*4	36	–	–	SWI/SNF	Hypothetical protein—31% glutamine
TTHERM_00129650	*SAF*3	24	–	–	SWI/SNF	Hypothetical protein—26% glutamine
TTHERM_00241840	*SAF*5	29	–	–	SWI/SNF	PHD finger-containing protein
TTHERM_00317000	Actin-like	63	–	–	Undefined	–
TTHERM_00046920	*RVB*2	174	893	–	SWR	–
TTHERM_00476820	*RVB*1	121	333	–	SWR	–
TTHERM_01546860	*SWR*1	113	561	–	SWR	–
TTHERM_00975380	Actin-like	101	542	–	SWR	–
TTHERM_01005190	*ARP*6	18	82	–	SWR	–
TTHERM_00170260	Sap3	23	144	–	SWR	Hypothetical protein
TTHERM_00357110	*SWC*4	33	419	–	SWR	–
TTHERM_00136450	*SWC*5/*AOR*1	32	121	–	SWR	Bucentaur or craniofacial development-containing protein
TTHERM_00355040	Sap1	20	78	–	SWR	AT-hook-containing protein
TTHERM_00388500	*SWC*2-like	19	75	–	SWR	–
TTHERM_00561450	*YAF*9	15	200	–	SWR	–
TTHERM_00046150	Sap2	9	32	–	SWR	Hypothetical protein
TTHERM_00978770	*TRA*1	–	767	–	Undefined	–
TTHERM_00979770	*TRA*2	–	179	–	Undefined	–
TTHERM_00444700	Aap1	51	–	356	SAGA	PHD finger-containing protein
TTHERM_00248390	*GCN*5	32	–	605	SAGA	–
TTHERM_00790730	*ADA*2	28	–	429	SAGA	–
TTHERM_00145290	Aap6	–	–	152	SAGA	–
TTHERM_00313140	Aap2	–	–	69	SAGA	PHD finger-containing protein

of Ibd1 is therefore correlated with transcriptionally active MAC during growth and nuclear development.

To determine whether Ibd1's protein interaction network changes during sexual development, we performed AP–MS using whole-cell extracts prepared from conjugating cells harvested 5 h post-mixing, a time period following meiosis that is marked by a series of rapid post-zygotic nuclear divisions and where Ibd1-FZZ is found exclusively in the parental MAC (Fig. 4b). SAINT-curated AP–MS data are shown in Additional

Table 3 continued

TTHERM	Gene name	Spectral count sum Ibd1 (BAIT)	Spectral count sum Swc4 (BAIT)	Spectral count sum Ada2 (BAIT)	Possible complex	Notes
TTHERM_00670640	Aap4	–	–	314	SAGA	PHD finger-containing protein
TTHERM_00502120	Aap3	–	–	184	SAGA	PHD finger-containing protein
TTHERM_00420400	Aap8	–	–	194	SAGA	–
TTHERM_00046390	Aap7	–	–	93	SAGA	–
TTHERM_00464970	Aap5	–	–	247	SAGA	–

Curated SAINTexpress data from 2 biological replicates of Ibd1-FZZ, Ada2-FZZ and Swc4-FZZ AP–MS samples

file 5. Direct comparison of the Ibd1 AP–MS results from vegetative and conjugating cells revealed that members of the SWI/SNF^{Tt} and the Atrx3^{Tt}/Set1^{Tt} HMT complexes were associated with Ibd1-FZZ to a lower degree in conjugation than during vegetative growth, while members of the putative SWR^{Tt} and SAGA^{Tt} remained relatively unaffected (Fig. 5a). The recovery as defined by spectral counts of SWI/SNF^{Tt} members (Fig. 3c; Tables 1, 3) appeared relatively low at this stage when compared to members of SWR^{Tt} and SAGA^{Tt}. To validate this finding, we used M2 agarose to affinity purify Ibd1-FZZ from untagged and Ibd1-FZZ-expressing cells and blotted with anti-Brg1 antibody following SDS-PAGE (Fig. 5b). In these conjugating cells, Ibd1-FZZ did not co-purify with Brg1^{Tt} (Fig. 5b), consistent with the substantially lower amounts of the protein detected by mass spectrometry. These data suggest a profound modulation of the Ibd1 interactome favoring its association with SWR^{Tt} and SAGA^{Tt} over SWI/SNF^{Tt} complex early in conjugation (5 h post-mixing).

Ibd1 localizes to transcriptionally active chromatin

As noted above, Ibd1 co-purifies with multiple protein complexes involved in gene expression regulation and in vitro recognizes histone marks associated with an active chromatin state. These observations suggest an intimate role of Ibd1 in transcription regulation. To examine this possibility in more detail, we employed chromatin immunoprecipitation followed by next-generation sequencing (ChIP-Seq). Specifically, we asked whether Ibd1 localizes to specific regions of the genome that correlate with transcriptionally active chromatin.

Data for two biological replicates that include DNA from input chromatin as well as Ibd1-FZZ precipitate from two independent experiments were analyzed. Our ChIP-Seq (GEO accession GSE103318) data set utilizing the available genome annotations [33] was composed of all annotated genic or open reading frames (ORF) and intergenic regions. The two generated lists displayed greater than or equal to twofold enrichment of Ibd1 and were ranked in descending order (see Additional files 6, 7, All_>2X_Fold_Enrichment tab). From these lists we observed that Ibd1 strongly occupies to 837 ORF and 396 intergenic regions with an enrichment (IP/INPUT) greater than or equal to twofold (Fig. 6a; see Additional files 6, 7, >2X_Enriched_with_Strong_Peaks tab). We initially focused our attention to the identified 837 ORFs and assessed the transcriptional state of these genes. We utilized previously published RNA-Seq data that have been used to rank genes based on their expression level during vegetative growth (GEO accession GSM692081 [43]). Based on these data we found that 9 and 29% of genes in *Tetrahymena* are highly and moderately expressed, respectively (Fig. 6b, left panel; see Additional file 6, RNA-Seq tab). On the other hand, we found that 54% (457 ORF) and 16% (134 ORF) of genes occupied by Ibd1 are highly and moderately expressed, respectively (Fig. 6b, right panel, c; see Additional file 6, localization tab). These observations are consistent with our histone peptide-array data and further strengthen the idea that Ibd1 primarily occupies active chromatin regions. Interestingly, Ibd1 showed binding to 114 ORF with low expression to no-expression during vegetative growth (Fig. 6c; see Additional file 6, localization tab). The overall trend of the Ibd1 binding pattern to highly expressed genes that are highly occupied is particularly evident for genes that have enrichment greater than or equal to fourfold (298 genes in total) (Fig. 6c). To examine whether these 298 genes are enriched for any particular functional categories, we grouped them using STRING [44] based on their predicted Gene Ontology (GO) terms [45]. We identified 122 genes that are significantly enriched with a particular term related to housekeeping functions, such as biological process, cellular process, translation, metabolic processes and gene expression (Fig. 6d, see Additional file 6, 4X+_GO_Biological_Expression tab). These housekeeping genes are generally highly expressed consistent with our findings that Ibd1 primarily occupies transcriptionally active chromatin. To compare these data with the overall distribution of all *Tetrahymena*'s

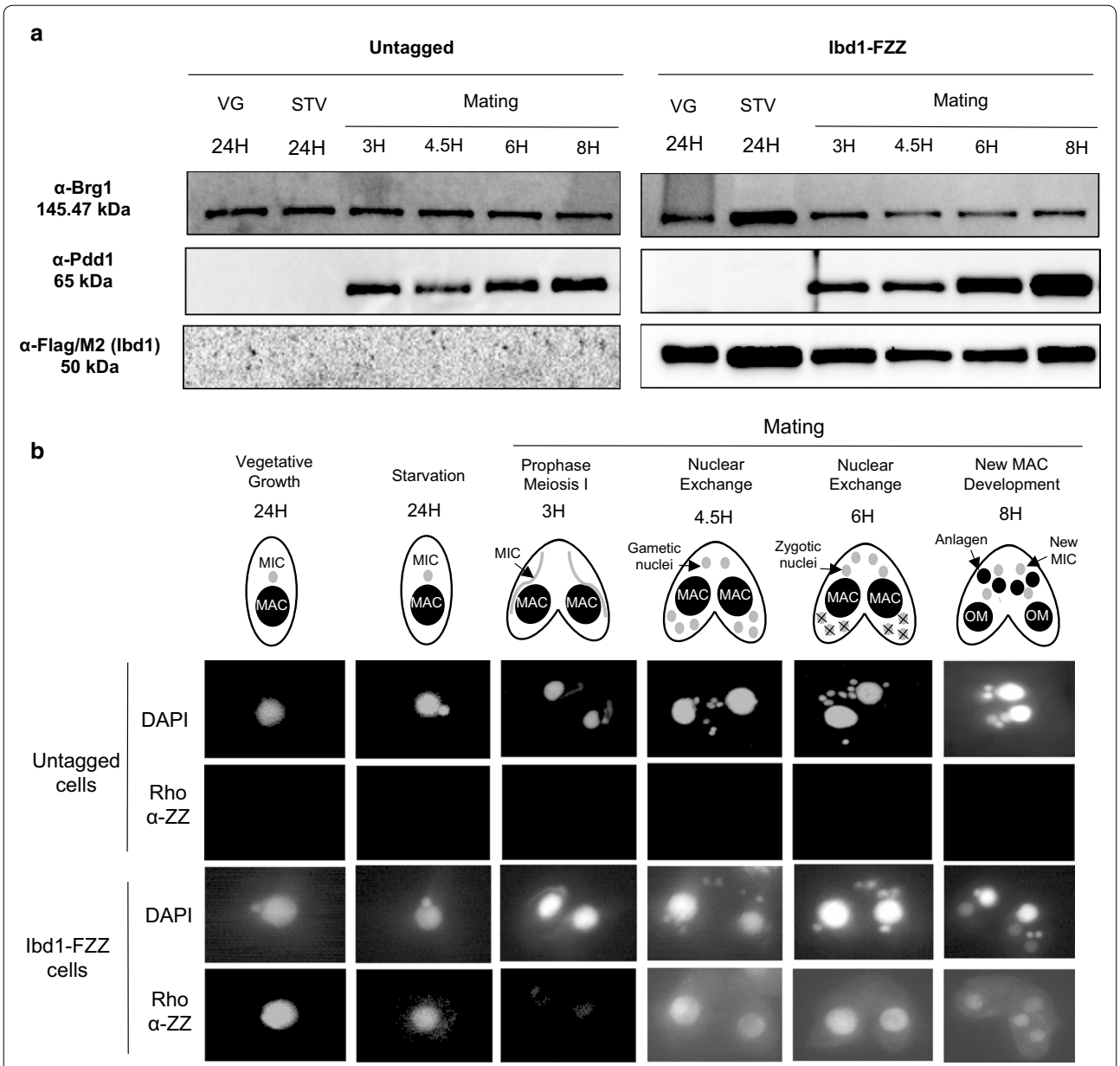

Fig. 4 Ibd1 expression pattern. Ibd1-FZZ (B2086) and untagged cells after 24 h of vegetative growth (VG) and starvation (STV) and after 3, 4, 5, 6 and 8 h post-mixing (mating of Ibd1-FZZ B2086 and CU428). **a** Expression analysis of Ibd1-FZZ during *T. thermophila*'s life cycle. Whole-cell extraction followed by TCA precipitation of untagged and tagged (Ibd1-FZZ) *Tetrahymena* strains. Ibd1 expresses throughout the *T. thermophila* life cycle (bottom panel). Brg1 is a loading control for expression throughout the *T. thermophila* life cycle (top panel). Pdd1 is an exclusively developmental protein and is used as a control during conjugation (middle panel); **b** Ibd1 localizes to the MAC during growth and sexual development including meiosis. The upper row of each panel shows a cartoon of *T. thermophila* depicting macronucleus (MAC), micronucleus (MIC), gametic nuclei, zygotic nuclei, new MIC, anlagen (new MAC) and old mac (OM) at different stages. Untagged cells are in the second and third panels and tagged (Ibd1-FZZ) are in the 2 lower panels. DAPI localizes to nuclei and Rho α-ZZ to the tagged protein

annotated genes the same approach was used (Fig. 6e; see Additional file 6, AllTtGenes_GO_Biological_Proces tab). Figure 6d, e suggests that Ibd1 mainly controls housekeeping genes in vegetative cells.

To validate our ChIP-Seq analysis of Ibd1-enriched chromatin, we designed primers for the three genes that showed the highest Ibd1-FZZ fold enrichment (see Additional file 6, >2X_Enriched_with_Strong_Peaks tab) as well as a fourth, *PDD1*, which is exclusively

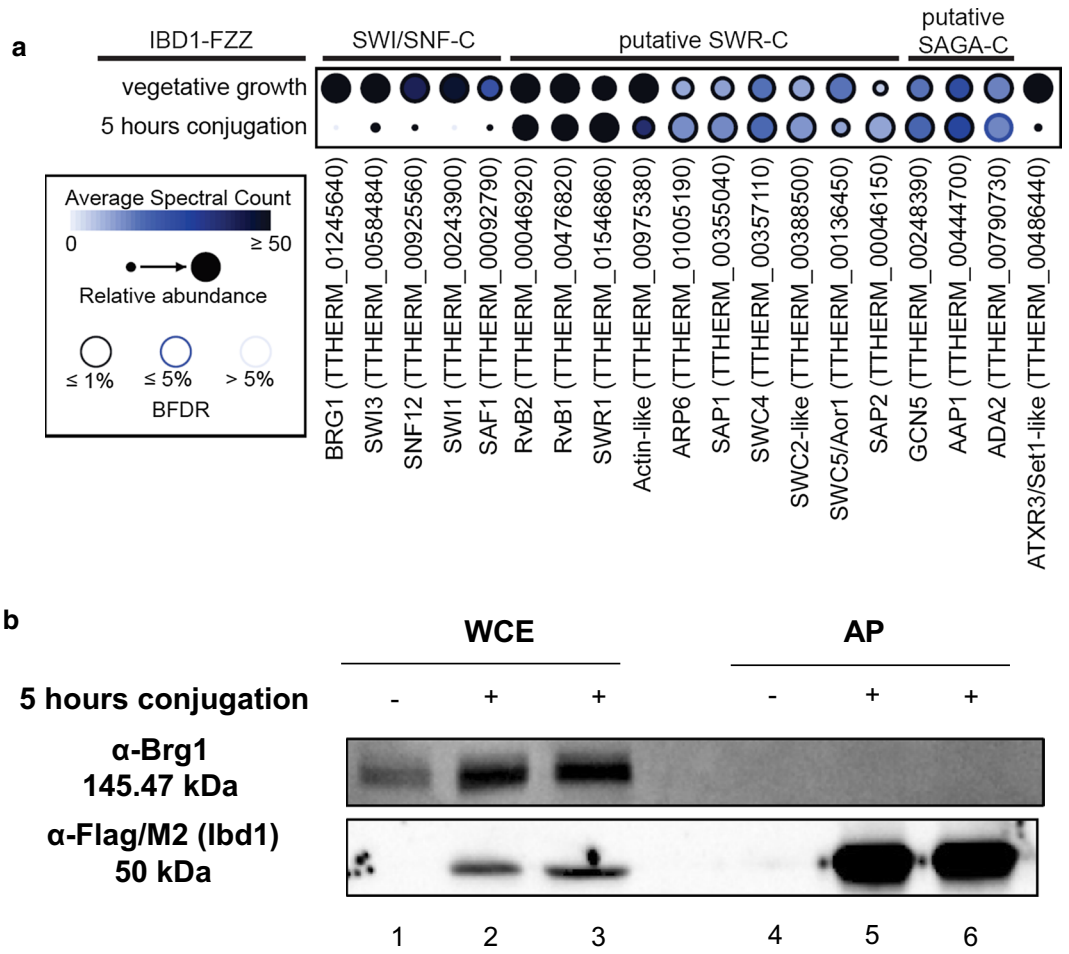

Fig. 5 **a** Modulation of Ibd1 interactome during conjugation. Dot plot overview of the interaction partners identified with Ibd1-FZZ during vegetative growth and 5 h after initiation of conjugation. Inner circle color represents the average spectral count, the circle size maps to the relative prey abundance across all samples shown, and the circle outer edge represents the SAINT FDR, **b** expression analysis of IBD1-FZZ 5 h into conjugation. Whole-cell extract (WCE) and affinity purification (AP) of untagged (−, lanes 1 and 4) and tagged (+, Ibd1-FZZ, lanes 2, 3, 5 and 6) strains. In the AP samples taken during conjugation Brg1 (top panel, lanes 5 and 6) and Pdd1p cannot be detected (data not shown). Ibd1 is recognized by α-FLAG/M2 (lower panel, lanes 5 and 6)

developmentally expressed [46] and did not show enrichment for Ibd1-FZZ during growth (see GEO accession GSE103318) (Table 4). Our ChIP-qPCR analysis of the four genes confirmed specific enrichment of Ibd1-FZZ in *HTA3*, *RPS22* and *HFF1* but not *PDD1* relative to chromatin made from untagged cells (Fig. 6f; see Additional file 8 for Raw data). We conclude that Ibd1 occupies transcriptionally active chromatin and might have a role in regulating the expression of a subset of genes involved in basal cellular housekeeping functions.

Localization of Ibd1 in *Tetrahymena*'s genome

We next examined our ChIP-Seq data for both ORFs and intergenic regions that showed greater than or equal to fourfold enrichment to determine how Ibd1 is situated in the genome relative to ORF and intergenic regions.

Using this fold-enrichment cutoff, we obtained 298 genic and 140 intergenic regions.

We first investigated the genic regions to assess the Ibd1 peak distribution. Figure 7a shows a representative example of Ibd1 ORF-specific localization where peaks are primarily enriched within the gene body (see Additional file 6, 4X_+_Ibd1_Occupancy tab for the full list). Next, to classify 140 intergenic regions, we manually inspected the ChIP-Seq peaks using the genome browser [47] and categorized them into five groups based on their localization (Fig. 7b–f; see Additional file 7, Intergenic_Groups tab). The promoter group showed intergenic localization that was proximal to the 5′ region of

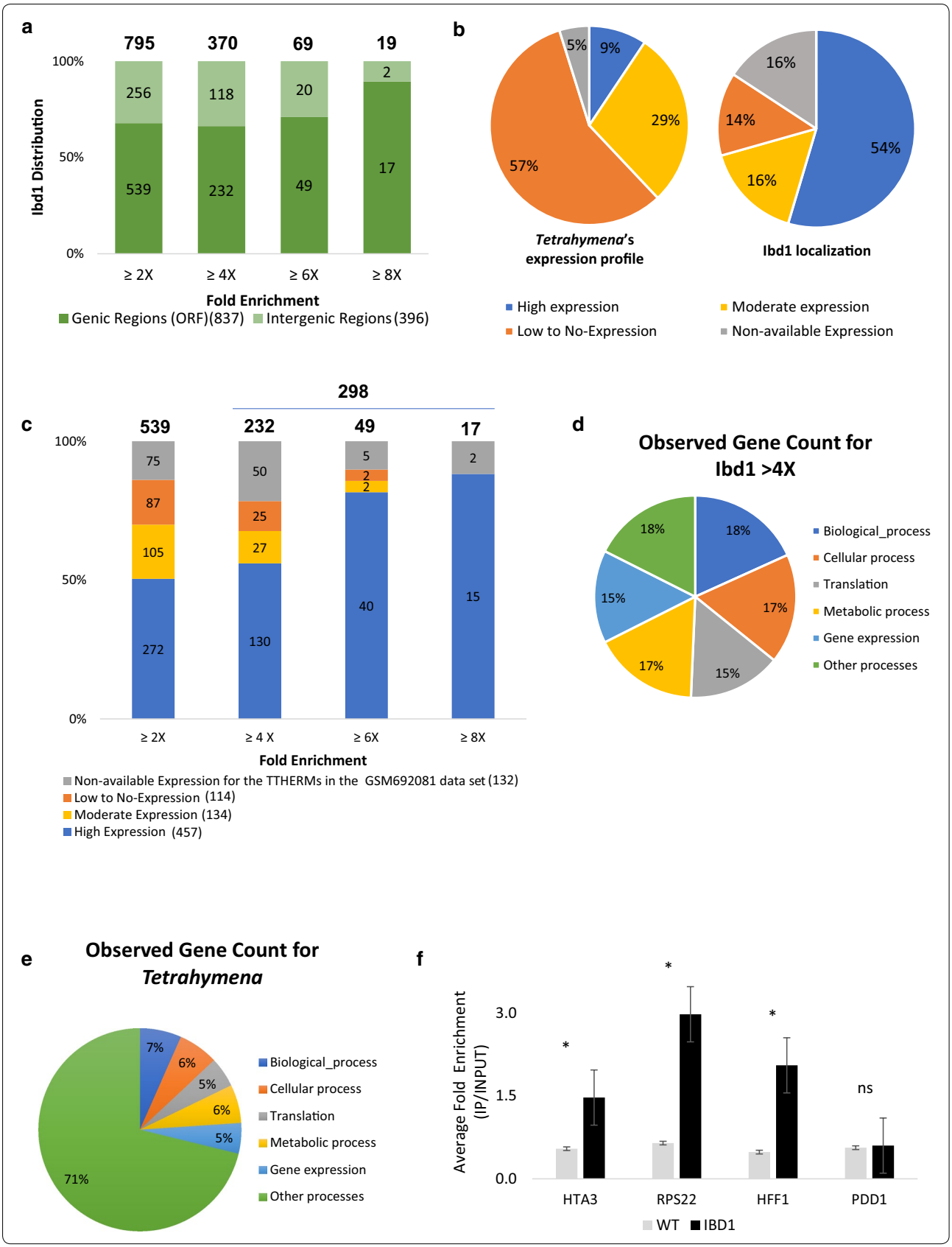
a
795
370
69
19
100%
50%
0%
Ibd1 Distribution
256
118
20
2
539
232
49
17
≥ 2X
≥ 4X
≥ 6X
≥ 8X
Fold Enrichment
Genic Regions (ORF)(837)
Intergenic Regions (396)
b
5%
9%
29%
57%
Tetrahymena's expression profile
16%
14%
54%
16%
Ibd1 localization
High expression
Moderate expression
Low to No-Expression
Non-available Expression
c
298
539
232
49
17
100%
50%
0%
75
87
105
272
50
25
27
130
5
2
2
40
2
15
≥ 2X
≥ 4 X
≥ 6X
≥ 8X
Fold Enrichment
Non-available Expression for the TTHERMs in the GSM692081 data set (132)
Low to No-Expression (114)
Moderate Expression (134)
High Expression (457)
d
Observed Gene Count for Ibd1 >4X
18%
18%
15%
17%
17%
15%
Biological_process
Cellular process
Translation
Metabolic process
Gene expression
Other processes
e
Observed Gene Count for Tetrahymena
7%
6%
5%
6%
5%
71%
Biological_process
Cellular process
Translation
Metabolic process
Gene expression
Other processes
f
Average Fold Enrichment (IP/INPUT)
3.0
1.5
0.0
*
*
*
ns
HTA3
RPS22
HFF1
PDD1
WT
IBD1

(See figure on previous page.)
Fig. 6 Ibd1 is localized to actively transcribed genes. **a** Ibd1 occupancy. Ibd1 shows occupancy for 837 ORF and 396 intergenic regions. When Ibd1 was enriched (IP/INPUT) 2–3 (≥ 2), 4–5 (≥ 4), 6–8 (≥ 6) and more than 8 (≥ 8) times it was found in 795, 370, 69 and 19 sites, respectively, **b** *Tetrahymena*'s expression distribution and Ibd1 localization. Left panel. 9% of *Tetrahymena*'s genes are highly expressed. Right panel. 457 ORF (54%) that are occupied by Ibd1 are highly expressed. Ibd1 also localizes to 132 (14%) coding regions that do not present available data for the RNA-Seq data (GEO accession GSM692081 [43]); **c** Ibd1 prefers highly expressed genes. High amounts of Ibd1 occupancy are related to highly expressed genes. The trend shows that the higher the Ibd1 fold enrichment (IP/INPUT) is the higher the occupancy of highly expressed genes. This is evident when Ibd1 is enriched more than 4 times; **d** Ibd1 frequently localizes to housekeeping genes. The GO terms of the observed genes with a significant enrichment (≥ 4) are genes responsible for cell maintenance, **e** *Tetrahymena*'s GO terms. Distribution of *T. thermophila* genes based on GO biological functions, **f** ChIP-qPCR validation. Anti-FLAG ChIP was performed in the 3 replicas of untagged and 4 replicas of Ibd1-FZZ during vegetative growth. ChIP DNA was amplified using primers to amplify *HTA*3, *RPS*22, *HFF*1 and *PDD*1 by real-time PCR using SYBR green. The significant *p* values from the *t* test are represented by a * (*p* value < 0.05). These significant *p* values are 0.043 for HTA3, 0.041 for RPS22 and 0.015 for HFF1; this confirmed enrichment of Ibd1 in these genes. Our negative control, Pdd1, shows no significant *p* value (ns) meaning no enrichment at this gene. The error bars represent the standard error of the mean for each sample (see Additional file 8 for Raw Data)

Table 4 Top Ibd1 ChIP-Seq hits during vegetative growth

TTHERM	Description	Fold enrichment	Highly expressed
TTHERM_00143660	Hta3_histone_H2A	12.75	Yes
TTHERM_00454080	Rps22_predicted_protein	9.50	Yes
TTHERM_00498190	Hhf1_predicted_protein	9.38	Yes
TTHERM_00125280	Pdd1_chromodomain_protein	1.00	No

The 3-top highly expressed genes and an exclusive developmental gene are shown

91 single predicted genes (e.g., Fig. 7b). The Ibd1 terminator group showed intergenic localization proximal to the 3′ region of 33 single predicted genes (e.g., Fig. 7c). The third intergenic group showed Ibd1 localization to 2 regions where there is an overlap between the promoter of one predicted gene and the terminator of another (e.g., Fig. 7d). The fourth group showed localization of Ibd1 to 13 single 5′ promoter regions potentially controlling expression of two predicted genes (Fig. 7e). The fifth group showed localization of Ibd1 to 11 single terminator 3′ regions of two distinct predicted genes (Fig. 7f). We found that among the 298 ORF showing ≥ 4X Ibd1 enrichment, 37 also additionally showed enrichment through the promoter (Fig. 7g; Additional file 7, Combining_Intergenic_and_ORF tab for list) and 19 at the terminator region (Fig. 7h; Additional file 7, Combining_Intergenic_and_ORF tab). Collectively these data suggest that Ibd1 appears to bind near the promoters and within gene bodies, consistent with a role in transcription regulation through its potential role in organizing multiple protein complexes.

Discussion

Ibd1 is a BRD-containing protein that interacts with multiple chromatin-remodeling complexes in *T. thermophila*

In our previous molecular characterization of Brg1^{Tt} [15], we reported that it lacked a C-terminal BRD which differs from the case in yeast (Snf2/Sth1) and mammalian cells (Brg1/Brahma). We report here that a distinct, BRD-containing protein, Ibd1, is a member of the *Tetrahymena* SWI/SNF complex. Recombinant Ibd1 recognized several Kac histone PTMs that are correlated with transcription. Ibd1 however established a large interaction network beyond the SWI/SNF^{Tt} complex including putative SAGA^{Tt} and SWR^{Tt} complexes as well a Atrx3/Set1-like HMT that is predicted to be H3K4 specific, a modification linked to transcription. As is standard practice, we used a promiscuous DNAse and RNAse (benzonase nuclease) in the preparation of whole-cell extracts used for AP–MS (as detailed in "Methods"). Very little, if any, nucleic acid remains in our extract submitted to AP–MS. Also, although Ibd1 AP–MS yielded several putative protein complexes, reciprocal purification of individual complex components co-purified Ibd1 but not the other complexes consistent with binding of other proteins to Ibd1 being specific and independent of DNA. This being said, we cannot exclude that nucleic acids already bound by proteins are protected from nuclease cleavage and may contribute to the observed binding events.

Characterization of a *Tetrahymena* SWI/SNF complex

The *Tetrahymena* SWI/SNF^{Tt} complex, as defined by the set of proteins that co-purify with Ibd1^{Tt}, Snf5^{Tt} and Saf5^{Tt}, includes orthologs of canonical SWI/SNF proteins Swi1, Swi3, Snf5, Snf12 and Snf2/Brg1, the PHD domain-containing Saf5, as well as several ciliate and species-specific novel proteins. Of note, three of the novel proteins

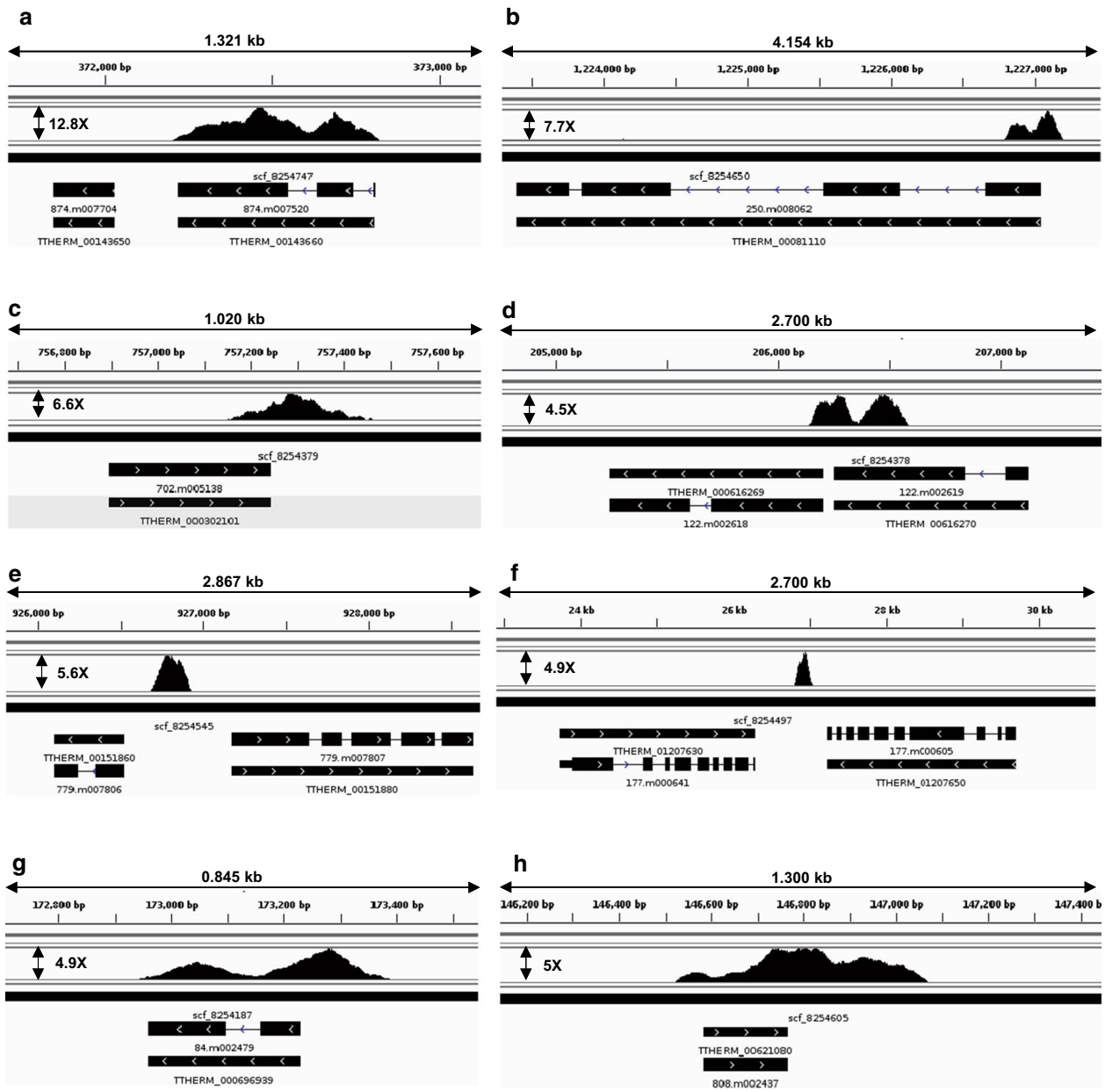

Fig. 7 Ibd1 is localized in promoters, ORF and terminators. In regions with more than or equal to fourfold enrichment (IP/NPUT), Ibd1 localizes to 8 specific type regions, including: **a** 483 ORF, **b** 91 promoters, **c** 33 terminators, **d** localization in 2 regions where there is overlap between the promoter of one predicted gene and the terminator of another, **e** 13 regions showed localization to a single 5′ promoter region potentially controlling expression of two predicted genes, **f** localization to 11 single terminator 3′ regions of two distinct predicted genes. Combining these data for genes that present enrichment in the ORF and intergenic region, we found that there is mutual enrichment in **g** 37 regions that occupy from the promoter to the ORF, and **h** 19 regions that present enrichment from the ORF to the terminator region (see Additional files 6, 7 for Raw Data). The fold enrichments are presented besides each peak

that co-purify with *Tetrahymena* SWI/SNF (Saf2^{Tt}, Saf3^{Tt} and Saf4^{Tt}) do not possess conserved domains outside of glutamine-rich regions. Yeast and mammalian Swi1^{Tt} possess an AT-rich interactive (ARID) and also a Q-rich domain [48]. Swi1^{Tt} possesses an ARID but not a Q-rich domain. We suggest that in SWI/SNF^{Tt}, the Q-rich proteins Saf2^{Tt}, Saf3^{Tt} and Saf4^{Tt} act in conjunction with Swi1^{Tt}. The Q-rich domain in animal Sp1 functions as an activation domain for transcription factors through recruitment of general transcription factor(s) [49]. We

suggest that the function of Saf2–4^{Tt} is to function in co-activation by recruiting general transcription factors and/or RNA polymerase to promoter regions of highly expressed genes in growing *Tetrahymena*.

The finding that Ibd1 is a member of SWI/SNF^{Tt} is informative in that its BRD interacts with Kac of histone proteins, similar to that observed for Snf2/Sth1 in yeast [50] and Brahma/Brg1 in humans [51]. In addition to the BRD-containing Ibd1, *Tetrahymena* SWI/SNF also contains a PHD domain-containing protein, Saf5^{Tt}. One function attributed to PHD domains is recognizing methylated lysines in proteins such as histones. For example the PHD domain of human ING2 recognizes H3K4me3 [25]. Thus, the SWI/SNF^{Tt} contains two proteins that potentially recognize PTM on histones, Saf5^{Tt} that likely recognizes methyl lysine (and possibly acetyl-lysine [27]) and Ibd1 that recognizes Kac. The *Tetrahymena* transcriptionally active MAC contains hyperacetylated histone H3 that is also di- or tri-methylated on H3K4 [40]. We suggest that a subset of these modified H3-containing nucleosomes can be recognized by SWI/SNF which would then remodel them to facilitate transcription. Additional SWI/SNF co-activator function could be derived from recruitment of general TFs and/or RNA polymerase II by the Saf2-4 proteins with Q-rich regions. Ibd1 may not interact with SWI/SNF in development in the same manner as it does during vegetative growth. We suggest that the function of SWI/SNF during nuclear development occurs independent of histone acetylation.

Tetrahymena Ibd1-containing SWR, SAGA and HMT complexes

In addition to being a member of SWI/SNF^{Tt}, Ibd1 is also a distinct component of the SWR and SAGA complexes as well as interacting with an uncharacterized H3K4-specific histone methyl transferase that is similar to human Atrx3 and yeast Set1. The function of the SWR complex in fission [52] and budding [6] yeasts is the deposition of the histone H2A variant Pht1/Htz1 (H2A.Z in humans and Hv1 in *Tetrahymena*). Deposition of Htz1 in budding yeast is linked to NuA4-dependent histone acetylation via the BRD-containing Bdf1 subunit of SWR [53]. In yeast, Bdf1 is also a component of TFIID linking histone acetylation to pre-initiation complex assembly [54]. In *Tetrahymena*, Ibd1 did not co-purify with any proteins similar to components of the general transcription apparatus. Like Ibd1, Hv1 is localized to transcriptionally active MAC in growing cells [55]. Unlike Ibd1, Hv1 localizes also to the crescent MIC corresponding to meiotic prophase [56], a time period in *Tetrahymena* where large genome-wide transcription of the MIC by RNAPII occurs (reviewed in [57]).

In budding yeast, SWR is functionally linked to the NuA4 histone acetyl transferase complex via shared subunits Swc4 and Yaf9. In *Tetrahymena,* Swc4^{Tt} did not co-purify with a histone acetyl transferase subunit and may not be a member of a NuA4-type complex. In fact, a strict NuA4-type complex in *Tetrahymena* is unlikely to exist, despite the presence of 3 genes encoding MYST family histone acetyl transferases. A previous study did identify a H2A/H4 nucleosomal HAT similar to the activity of NuA4 but also showed by glycerol gradient analysis that the activity purifies at ~80 kDa [58]. Consistent with this observation, the MAC does not appear to encode a gene that is a clear ortholog of the conserved NuA4 subunit such as Epl1/EPC so it is unclear whether there exists a 'piccolo' NuA4 [59]. Swc4^{Tt} did co-purify with orthologs of Tra1^{Tt} and Tra2^{Tt} kinases that did not purify with Ibd1 (Table 3; Fig. 3c). In *S. cerevisiae* Tra1 co-purifies with NuA4 [60] and SAGA [61] that contribute to their co-activator function [62]. It will be interesting to determine whether SAGA^{Tt} fulfills the function of SAGA and NuA4 in budding yeast or whether there exists a divergent version of NuA4 in *Tetrahymena*.

Ibd1 co-purifies with Gcn5^{tt} and Ada2^{Tt} in addition to the PHD domain-containing A2A1^{Tt}. Ada2^{Tt} co-purifies with these proteins in addition to seven others including three additional PHD domain-containing proteins A2A2-4^{Tt}. Thus, Ada2^{Tt} co-purifies with four distinct PHD domain-containing proteins. Further work will be necessary to determine whether the set of Ada2-interacting proteins represent a single assemblage or whether Ibd1, Ada2 and Gcn5 represent a 'core' to the *Tetrahymena* SAGA complex that can have different specificity depending on which PHD protein it is interacting with at a particular time.

Model for Ibd1 function

We hypothesize that Ibd1 has a common function that it performs in diverse chromatin-remodeling complexes. Consistent with a function in promoting transcription, Ibd1-FZZ specifically localized to the coding regions of multiple highly transcribed genes during vegetative growth. A model for Ibd1 function is that it recognizes one or more specific histone Kac marks that are associated with transcription and recruits multiple chromatin-related complexes to the region to either further acetylate nearby chromatin (SAGA^{Tt}), to remodel nucleosomes (SWI/SNF^{Tt}), to deposit Hv1 (SWR^{Tt}), and to di- or tri-methylate histone H3K4 (Atrx3/Set1-like histone methyl transferase). SWI/SNF, SAGA and SWR, and H3K4 methylation are all linked to transcription in other experimental systems. We predict that Ibd1 is particularly important to maintain high rates of transcription on highly expressed genes such as those encoding

the core histones or ribosomal proteins. Our ChIP-Seq analysis of Ibd1 supports this hypothesis with strong occupancy of the coding regions of genes encoding core histones HHT1 and HHF1. ChIP-Seq of Ibd1-containing complex-specific members (i.e., $Snf5^{Tt}$, $Swr1^{Tt}$, $Ada2^{Tt}$) will be required to test the validity of this hypothesis. As well as being found in coding regions, Ibd1 also localizes to the regulatory region of several genes. Further work will be necessary to determine whether Ibd1 is necessary for the recruitment of SWI/SNF^{Tt}, $SAGA^{Tt}$, SWR^{Tt} and the HMT to ORFs and the regulatory regions identified in our ChIP-Seq analysis. It will also be interesting to determine whether the regulatory regions enriched in Ibd1 contain conserved DNA sequences that may indicate whether specific DNA-binding transcription factors recruit Ibd1-containing protein complexes to regulatory regions.

BRD proteins in *Tetrahymena*

We have identified and performed a phylogenetic analysis on 14 BRD-containing proteins in *Tetrahymena*. Ibd1 is a member of a grouping that includes six proteins, five of which are like Ibd1 in possessing a single BRD and no other recognizable domains. Four of these 5 are similar in length to Ibd1 suggesting relatively recent evolutionary divergence of the four. BRD inhibitors are currently of a significant clinical interest in the development of drugs to treat parasitic infections as a number of apicomplexan protozoan parasites possess lineage-specific BRD proteins that appear to be important for various stages of their life cycle [63]. Because the ciliates and apicomplexans are closely related in evolution, we suggest *Tetrahymena* may provide a tractable model for molecular analysis of some of these BRD proteins.

Conclusions

In multi-cellular eukaryotes, the precise function of how chromatin-remodeling complexes work is poorly understood. Alteration or loss of factors involved in these complexes through mutation has been shown to be associated with cancer. We utilized the protist model, the Aleveloate *Tetrahymena thermophila* which segregates transcriptionally active, and silent chromatin into two distinct nuclei, the macronucleus (MAC) and micronucleus (MIC), respectively, contained in the same cell. Through the discovery of a bromodomain-containing protein, Ibd1, we advanced the knowledge of chromatin-remodeling complexes in protists by defining for the first time the protein complements of SWI/SNF, SWR and SAGA complexes. In addition, we present a model where a single protein, Ibd1, coordinates the action of multiple chromatin-remodeling complexes to achieve high levels of transcription. Our research will contribute to our current understanding of transcription in ciliates, and more broadly the function and diversity of chromatin-remodeling complexes in eukaryotes.

Methods

Protein sequence alignments

Multiple sequence alignments of Snf5, Saf5 and Ibd1 amino acid sequence from various model organisms were performed using Clustal Omega (http://www.ebi.ac.uk/Tools/msa/clustalo/) and then shaded by importing the ALN file into the Boxshade server (http://www.ch.embnet.org/software/BOX_form.html). SMART [64] was used to find the beginning and end of the domains.

Cell strains

Tetrahymena thermophila strains CU428 [Mpr/Mpr (VII, mp-s)] and B2086 [Mpr+/Mpr+ (II, mp-s)] of inbreeding line B were obtained from the *Tetrahymena* Stock Center, Cornell University, Ithaca, NY (http://tetrahymena.vet.cornell.edu/). Cells were cultured axenically in 1 × SPP at 30 °C as previously described [65].

Oligonucleotides

See Additional file 9 for a list of the oligonucleotides used during this study.

DNA manipulations

Whole-cell DNA was isolated from *T. thermophila* strains as described [66]. Molecular biology techniques were carried out using standard protocols or by following a supplier's instructions.

Affinity purification, sample preparation and mass spectrometric analysis

AP–MS analysis was performed as per [21] with minor modifications, see Additional file 10.

Macronuclear gene replacement

Epitope-tagging vectors for Snf5, Saf5, Ibd1, Swc4 and Ada2 were constructed as previously described [21].

ChIP

ChIP was performed as described [67] with modifications described in Additional file 10.

NGS

Sequencing and analysis of DNA co-purifying with ChIP of Ibd1-FZZ is described in Additional file 10.

ChIP-qPCR

Four ChIP biological repetitions for the Ibd1-FZZ and three ChIP repetitions for the untagged cell lines were quantified (NanoDrop, Thermo Scientific) and diluted to reach the smallest DNA concentration found in a

sample (1–3.1 ng/μL of DNA). Master mixes with a final volume of 20 μL were prepared (SYBR Green Supermix, Cat. #1708880, Bio-Rad) to amplify: the top 3 genes that presented the highest fold enrichment from Ibd1-FZZ ChIP-Seq and are highly expressed and a gene that is not expressing during vegetative growth (*PDD1*) (primers, see Additional file 9) using qPCR (CFX 96-well Real-Time System, Bio-Rad) with the following parameters: initial denaturation at 98 °C for 3 min; 40 cycles of amplification at 95 °C for 15 s and 60 °C for 60 s followed by acquisition in the SYBR/FAM channel; and melting curve from 65 to 95 °C increasing 0.5 °C/cycle and acquisition every 0.5 s in the SYBR/FAM channel. Each targeted gene was considered as an individual experiment each with its own standard curve. The standard curve for each target has 3 points representing 100, 10 and 1% of the corresponding input sample. The largest point of the curve was undiluted input sample and was followed by serial dilutions (see Additional file 8). Raw Cq values for input DNA and IP DNA were analyzed using the Bio-Rad Prime PCR program, which normalizes these data to the generated standard curve that we represented as % with respect to the INPUT. Ultimately, these normalized ChIP data are expressed as fold enrichment, by dividing normalized IP over normalized Input. The standard error of the mean (SEM) was calculated for each duplicate (see Additional file 8).

Additional experimental procedures can be accessed in Additional file 10.

Additional files

Additional file 1. Snf5_Alignments_Cloning.

Additional file 2. Saf5_Alignments_Cloning.

Additional file 3. Ibd1_Alignments_Cloning.

Additional file 4. Peptide_array.

Additional file 5. Ibd1_MS_5hConj.

Additional file 6. ChIP_seq_ORF.

Additional file 7. ChIP_seq_Intergenic.

Additional file 8. ChIP_qPCR.

Additional file 9. Primers.

Additional file 10. Additional_Methods.

Authors' contributions

AS generated Ibd1-FZZ, Saf5-FZZ and 6xHIS-Ibd1 cell lines and performed immunoprecipitations, affinity purifications, peptide array, IF microscopy for Ibd1-FZZ and Saf5-FZZ, ChIP-Seq, ChIP-qPCR, Western Blots, prepared figures and wrote manuscript. JG generated Snf5-FZZ, Swc4-FZZ, Ada2-FZZ cell lines and performed IF microscopy for Snf5-FZZ. JPL processed and analyzed samples for mass spectrometry, generated figures, participated in writing the manuscript and editing. SNS performed bioinformatics analyses of bromodomains in *T. thermophila*. MP participated in processing and analysis of ChIP-Seq data. AB participated in peptide array and IF, and CTM participated in ChIP-Seq. ACG and RP were responsible for supervision and manuscript editing. JF conceived the study, participated in its design and coordinated and edited the manuscript. All authors read and approved the final manuscript.

Author details

[1] Department of Chemistry and Biology, Ryerson University, 350 Victoria St., Toronto M5B 2K3, Canada. [2] Department of Biology, York University, 4700 Keele St., Toronto M3J 1P3, Canada. [3] Lunenfeld-Tanenbaum Research Institute at Mount Sinai Hospital, Toronto M5G 1X5, Canada. [4] SciNet HPC Consortium, University of Toronto, 661 University Ave, Suite 1140, Toronto M5G 1M1, Canada. [5] Department of Molecular Genetics, University of Toronto, Toronto M5S 1A8, Canada. [6] Department of Molecular Medicine, Université Laval, Quebec, Canada. [7] Centre Hospitalier Universitaire de Québec Research Center, CHUL, 2705 Boulevard Laurier, Quebec, G1V 4G2, Canada. [8] Present Address: Department of Molecular Genetics, University of Toronto, Toronto M5S 1A8, Canada.

Acknowledgements

We acknowledge Saba Zafar and Camila Imamura for technical expertise.

Competing interests

The authors declare that they have no competing interests.

Availability of data and materials

Mass spectrometry data have been deposited in the Mass spectrometry Interactive Virtual Environment (MassIVE, http://massive.ucsd.edu) MSV000081461. All MS files used in this study were deposited at MassIVE (http://massive.ucsd.edu) and were assigned the MassIVE identifier MSV000081461. Direct link to MassIVE data set: http://massive.ucsd.edu/ProteoSAFe/dataset.jsp?task=75098964a529429c943dac8a9ae537f7. ChIP-Seq data generated in this paper can be found online at Gene Expression Omnibus (GEO, http://www.ncbi.nlm.nih.gov/geo/) GSE103318. NGS and peak files produced in this study were deposited at https://www.ncbi.nlm.nih.gov/geo/ with unique identifier GSE103318. Direct link: http://www.ncbi.nlm.nih.gov/geo/query/acc.cgi?acc=GSE103318.

Consent for publication

Not applicable.

Ethics approval and consent to participate

Not applicable.

Funding

Work in the Fillingham and Lambert laboratory was supported by Natural Sciences and Engineering Research Council of Canada (NSERC) Discovery Grants RGPIN-2015-06448 and 1304616, respectively. Work in the Pearlman laboratory was supported by Canadian Institutes of Health Research (CIHR) MOP13347 and Natural Sciences and Engineering Research Council of Canada (NSERC) Discovery Grant 539509. Work in the Gingras laboratory was supported by the Canadian Institutes of Health Research (CIHR) Foundation Grant (FDN 143301). Proteomics work was performed at the Network Biology Collaborative Centre at the Lunenfeld-Tanenbaum Research Institute, a facility supported by Canada Foundation for Innovation funding, by the Ontarian Government and by Genome Canada and Ontario Genomics. A.-C.G. is the Canada Research Chair (Tier 1) in Functional Proteomics. J.-P.L. was funded by a Scholarship for the Next Generation of Scientists from the Cancer Research Society. SciNet is funded by: the Canada Foundation for Innovation under the auspices of Compute Canada; the Government of Ontario; Ontario Research Fund—Research Excellence; and the University of Toronto.

Publisher's Note

Received: 1 December 2017 Accepted: 27 February 2018
Published online: 09 March 2018

References

1. Hassan AH, Prochasson P, Neely KE, Galasinski SC, Chandy M, Carrozza MJ, et al. Function and selectivity of bromodomains in anchoring

chromatin-modifying complexes to promoter nucleosomes. Cell. 2002;111:369–79.
2. Jain AK, Barton MC. Bromodomain histone readers and cancer. J Mol Biol. 2017;429:2003–10.
3. Ginsburg DS, Anlembom TE, Wang J, Patel SR, Li B, Hinnebusch AG. NuA4 links methylation of histone H3 lysines 4 and 36 to acetylation of histones H4 and H3. J Biol Chem. 2014;289:32656–70.
4. Strahl BD, Grant PA, Briggs SD, Sun Z-W, Bone JR, Caldwell JA, et al. Set2 Is a nucleosomal histone H3-selective methyltransferase that mediates transcriptional repression. Mol Cell Biol. 2002;22:1298–306.
5. Steunou A-L, Cramet M, Rossetto D, Aristizabal MJ, Lacoste N, Drouin S, et al. Combined action of histone reader modules regulates NuA4 local acetyltransferase function but not its recruitment on the genome. Mol Cell Biol. 2016;36:2768–81.
6. Krogan NJ, Keogh M-C, Datta N, Sawa C, Ryan OW, Ding H, et al. A Snf2 family ATPase complex required for recruitment of the histone H2A variant Htz1. Mol Cell. 2003;12:1565–76.
7. Kobor MS, Venkatasubrahmanyam S, Meneghini MD, Gin JW, Jennings JL, Link AJ, et al. A protein complex containing the conserved Swi2/Snf2-related ATPase Swr1p deposits histone variant H2A.Z into euchromatin. PLoS Biol. 2004;2:e131.
8. Papamichos-chronakis M, Watanabe S, Rando OJ, Craig L. Global regulation of H2A.Z localization by the INO80 chromatin remodeling enzyme is essential for genome integrity. Cell. 2011;144:200–13.
9. Martindale DW, Allis CD, Bruns PJ. Conjugation in *Tetrahymena thermophila*. A temporal analysis of cytological stages. Exp Cell Res. 1982;140:227–36.
10. Yao M, Choi J, Yokoyama S, Austerberry CF, Yao C. DNA elimination in Tetrahymena: a developmental process involving extensive breakage and rejoining of DNA at defined sites. Cell. 1984;36:433–40.
11. Chalker DL, Yao MC. Nongenic, bidirectional transcription precedes and may promote developmental DNA deletion in *Tetrahymena thermophila*. Genes Dev. 2001;15:1287–98.
12. Schoeberl UE, Kurth HM, Noto T, Mochizuki K. Biased transcription and selective degradation of small RNAs shape the pattern of DNA elimination in Tetrahymena. Genes Dev. 2012;26:1729–42.
13. Mochizuki K, Gorovsky MA. RNA polymerase II localizes in *Tetrahymena thermophila* meiotic micronuclei when micronuclear transcription associated with genome rearrangement occurs. Eukaryot Cell. 2004;3:1233–40.
14. Gao S, Liu Y. Intercepting noncoding messages between germline and soma. Genes Dev. 2012;26:1774–9.
15. Fillingham J, Garg J, Tsao N, Vythilingum N, Nishikawa T, Pearlman RE. Molecular genetic analysis of an SNF2/brahma-related gene in *Tetrahymena thermophila* suggests roles in growth and nuclear development. Eukaryot Cell. 2006;5:1347–59.
16. Laurent BC, Treich I, Carlson M. The yeast SNF2/SWI2 protein has DNA-stimulated ATPase activity required for transcriptional activation. Genes Dev. 1993;7:583–91.
17. Wang W, Cote J, Xue Y, Zhou S, Khavari PA, Biggar SR, et al. Purification and biochemical heterogeneity of the mammalian SWI-SNF complex. EMBO J. 1996;15:5370–82.
18. Phelan M, Sif S, Narlikar G, Kingston R. Reconstitution of a core chromatin remodeling complex from SWI/SNF subunits. Mol Cell. 1999;3:247–53.
19. Chalker DL. Transformation and strain engineering of *Tetrahymena*. Methods Cell Biol. 2012;109:327–45.
20. Min B, Collins K. An RPA-related sequence-specific DNA-binding subunit of telomerase holoenzyme is required for elongation processivity and telomere maintenance. Mol Cell. 2010;36:609–19.
21. Garg J, Lambert J-P, Karsou A, Marquez S, Nabeel-Shah S, Bertucci V, et al. Conserved Asf1-importin β physical interaction in growth and sexual development in the ciliate *Tetrahymena thermophila*. J Proteom. 2013;94C:311–26.
22. Cassidy-Hanley D, Bowen J, Lee JH, Cole E, Verplank LA, Gaertip J, et al. Germline and somatic transformation of mating *Tetrahymena thermophila* by particle bombardment. Genet Soc Am. 1997;146:135–47.
23. Karrer KM. Nuclear dualism. Methods Cell Biol. 2012;109:29–52.
24. Teo G, Liu G, Zhang J, Nesvizhskii AI, Gingras AC, Choi H. SAINTexpress: improvements and additional features in Significance Analysis of INTeractome software. J Proteom. 2014;100:37–43.
25. Shi X, Hong T, Walter KL, Ewalt M, Michishita E, Hung T, et al. ING2 PHD domain links histone H3 lysine 4 methylation to active gene repression. Nature. 2006;442:96–9.
26. Kadoch C, Crabtree GR. Mammalian SWI/SNF chromatin remodeling complexes and cancer: mechanistic insights gained from human genomics. Sci Adv. 2015;1:e1500447.
27. Lange M, Kaynak B, Forster UB, Tönjes M, Fischer JJ, Grimm C, et al. Regulation of muscle development by DPF3, a novel histone acetylation and methylation reader of the BAF chromatin remodeling complex. Genes Dev. 2008;22:2370–84.
28. Williams NE, Hontst JE. Isolation and fractionation of the tetrahymena cytoskeleton and oral apparatus. Methods Cell Biol. 1995;47:301–6.
29. Mellacheruvu D, Wright Z, Couzens AL, Lambert J, St-denis N, Li T, et al. The CRAPome: a contaminant repository for affinity purification mass spectrometry data. Nat Methods. 2013;10:730–6.
30. Seipel K, Georgiev O, Schaffner W. Different activation domains stimulate transcription from remote ('enhancer') and proximal ('promoter') positions. EMBO. 1992;11:4961–8.
31. Muller S, Filippakopoulos P, Knapp S. Bromodomains as therapeutic targets. Expert Rev Mol Med. 2011;13:e29.
32. Fujisawa T, Filippakopoulos P. Functions of bromodomain-containing proteins and their roles in homeostasis and cancer. Mol Cell Biol. 2017;18:246–62.
33. Stover NA, Krieger CJ, Binkley G, Dong Q, Fisk DG, Nash R, et al. Tetrahymena Genome Database (TGD): a new genomic resource for *Tetrahymena thermophila* research. Nucleic Acids Res. 2006;34:D500–3.
34. Filippakopoulos P, Picaud S, Mangos M, Keates T, Lambert JP, Barsyte-Lovejoy D, et al. Histone recognition and large-scale structural analysis of the human bromodomain family. Cell. 2012;149:214–31.
35. Berkovits BD, Wolgemuth DJ. The role of the double bromodomain-containing BET genes during mammalian spermatogenesis. Curr Top Dev Biol. 2013;102:293–326.
36. Taniguchi Y. The bromodomain and extra-terminal domain (BET) family: functional anatomy of BET paralogous proteins. Int J Mol Sci. 2016;17:1–24.
37. Rahman S, Sowa ME, Ottinger M, Smith JA, Shi Y, Harper JW, et al. The Brd4 extraterminal domain confers transcription activation independent of pTEFb by recruiting multiple proteins, including NSD3. Mol Cell Biol. 2011;31:2641–52.
38. Filippakopoulos P, Knapp S. Targeting bromodomains: epigenetic readers of lysine acetylation. Nat Rev Drug Discov. 2014;13:337–56.
39. Chicoine LG, Richman R, Cook RG, Gorovsky MA, Allis CD. A single histone acetyltransferase from *Tetrahymena macronuclei* catalyzes deposition-related acetylation of free histones and transcription-related acetylation of nucleosomal histones. J Cell Biol. 1987;105:127–35.
40. Taverna SD, Ueberheide BM, Liu Y, Tackett AJ, Diaz RL, Shabanowitz J, et al. Long-distance combinatorial linkage between methylation and acetylation on histone H3N termini. Proc Natl Acad Sci USA. 2007;104:2086–91.
41. Sampath SC, Marazzi I, Yap KL, Sampath SC, Krutchinsky AN, Mecklenbräuker I, et al. Methylation of a histone mimic within the histone methyltransferase G9a regulates protein complex assembly. Mol Cell. 2007;27:596–608.
42. Madireddi MT, Coyne RS, Smothers JF, Mickey KM, Yao MC, Allis CD. Pdd1p, a novel chromodomain-containing protein, links heterochromatin assembly and DNA elimination in Tetrahymena. Cell. 1996;87:75–84.
43. Xiong J, Lu X, Zhou Z, Chang Y, Yuan D, Tian M, et al. Transcriptome analysis of the model protozoan, *Tetrahymena thermophila*, using deep RNA sequencing. PLoS ONE. 2012;7:1–13.
44. Snel B, Lehmann G, Bork P, Huynen MA. STRING: a web-server to retrieve and display the repeatedly occurring neighbourhood of a gene. Nucleic Acids Res. 2000;28:3442–4.
45. Gene Ontology C. Gene ontology: tool for the identification of biology. Nat Genet. 2000;25:25–9.
46. Smothers JF, Mizzen CA, Tubbert MM, Cook RG, Allis CD. Pdd1p associates with germline-restricted chromatin and a second novel anlagen-enriched protein in developmentally programmed DNA elimination structures. Development. 1997;124:4537–45.
47. Robinson JT, Thorvaldsdóttir H, Winckler W, Guttman M, Lander ES, Getz G, et al. Integrative genomics viewer. Nat Biotechnol. 2011;29:24–6.

48. Mao X, Cao F, Nie X, Liu H, Chen J. The Swi/Snf chromatin remodeling complex is essential for hyphal development in *Candida albicans*. FEBS Lett. 2006;580:2615–22.
49. Emili A, Greenblatt J, Ingles CJ. Species-specific interaction of the glutamine-rich activation domains of Sp1 with the TATA box-binding protein. Mol Cell Biol. 1994;14:1582–93.
50. Hassan AH, Awad S, Al-Natour Z, Othman S, Mustafa F, Rizvi TA. Selective recognition of acetylated histones by bromodomains in transcriptional co-activators. Biochem J. 2007;402:125–33.
51. Shen W, Xu C, Huang W, Zhang J, Carlson JE, Tu X, et al. Solution structure of human Brg1 bromodomain and its specific binding to acetylated histone tails. Biochemistry. 2007;46:2100–10.
52. Kim H, Vanoosthuyse V, Fillingham J, Roguev A, Watt S, Kislinger T, et al. An acetylated form of histone H2A.Z regulates chromosome architecture in *Schizosaccharomyces pombe*. Nat Struct Mol Biol. 2009;16:1286–93.
53. Raisner RM, Hartley PD, Meneghini MD, Bao MZ, Liu CL, Schreiber SL, et al. Histone variant H2A.Z marks the 5′ ends of both active and inactive genes in euchromatin. Cell. 2005;123:233–48.
54. Matangkasombut O, Buratowski RM, Swilling NW, Buratowski S. Bromodomain factor 1 corresponds to a missing piece of yeast TFIID. Genes Dev. 2000;14:951–62.
55. Allis CD, Richman R, Gorovsky MA, Ziegler YS, Touchstone B, Bradley WA, et al. hv1 is an evolutionarily conserved H2A variant that is preferentially associated with active genes. J Biol Chem. 1986;261:1941–8.
56. Stargell LA, Bowen J, Dadd CA, Dedon PC, Davis M, Cook RG, et al. Temporal and spatial association of his tone H2A variant hv1 with transcriptionally competent chromatin during nuclear development in *Tetrahymena thermophila*. Genes Dev. 1993;7:2641–51.
57. Schoeberl UE, Mochizuki K. Keeping the soma free of transposons: programmed DNA elimination in ciliates. J Biol Chem. 2011;286:37045–52.
58. Ohba R, Steger DJ, Brownell JE, Mizzen CA, Cook RG, Côté J, et al. A novel H2A/H4 nucleosomal histone acetyltransferase in *Tetrahymena thermophila*. Mol Cell Biol. 1999;19:2061–8.
59. Chittuluru JR, Chaban Y, Monnet-Saksouk J, Carrozza MJ, Sapountzi V, Selleck W, et al. Structure and nucleosome interaction of the yeast NuA4 and Piccolo-NuA4 histone acetyltransferase complexes. Nat Struct Mol Biol. 2012;18:1196–203.
60. Allard S, Utley RT, Savard J, Clarke A, Grant P, Brandl CJ, et al. NuA4, an essential transcription adaptor/histone H4 acetyltransferase complex containing Esa1p and the ATM-related cofactor Tra1p. EMBO J. 1999;18:5108–19.
61. Grant PA, Schieltz D, Pray-Grant MG, Yates JR III, Workman JL. The ATM-related cofactor Tra1 is a component of the purified SAGA complex. Mol Cell. 1998;2:863–7.
62. Knutson BA, Hahn S. Domains of Tra1 important for activator recruitment and transcription coactivator functions of SAGA and NuA4 complexes. Mol Cell Biol. 2011;31:818–31.
63. Jeffers V, Yang C, Huang S, Sullivan WJ. Bromodomains in protozoan parasites: evolution, function, and opportunities for drug development. Microbiol Mol Biol Rev. 2017;81:e00047-16.
64. Schultz J, Milpetz F, Bork P, Ponting CP. SMART, a simple modular architecture research tool: identification of signaling domains. Proc Natl Acad Sci USA. 1998;95:5857–64.
65. Fillingham JS, Bruno D, Pearlman RE. Cis-acting requirements in flanking DNA for the programmed elimination of mse2.9: a common mechanism for deletion of internal eliminated sequences from the developing macronucleus of *Tetrahymena thermophila*. Nucleic Acids Res. 2001;29:488–98.
66. Fillingham JS, Pearlman RE. Role of micronucleus-limited DNA in programmed deletion of mse2.9 during macronuclear development of *Tetrahymena thermophila*. Eukaryot Cell. 2004;3:288–301.
67. Fillingham J, Kainth P, Lambert JP, van Bakel H, Tsui K, Peña-Castillo L, et al. Two-color cell array screen reveals interdependent roles for histone chaperones and a chromatin boundary regulator in histone gene repression. Mol Cell. 2009;35:340–51.